



Centrality and rapidity dependence of inclusive jet production in $\sqrt{s_{NN}} = 5.02$ TeV proton–lead collisions with the ATLAS detector



ATLAS Collaboration*

ARTICLE INFO

Article history:

Received 12 December 2014

Received in revised form 16 April 2015

Accepted 14 July 2015

Available online 17 July 2015

Editor: D.F. Geesaman

ABSTRACT

Measurements of the centrality and rapidity dependence of inclusive jet production in $\sqrt{s_{NN}} = 5.02$ TeV proton–lead ($p + Pb$) collisions and the jet cross-section in $\sqrt{s} = 2.76$ TeV proton–proton collisions are presented. These quantities are measured in datasets corresponding to an integrated luminosity of 27.8 nb^{-1} and 4.0 pb^{-1} , respectively, recorded with the ATLAS detector at the Large Hadron Collider in 2013. The $p + Pb$ collision centrality was characterised using the total transverse energy measured in the pseudorapidity interval $-4.9 < \eta < -3.2$ in the direction of the lead beam. Results are presented for the double-differential per-collision yields as a function of jet rapidity and transverse momentum (p_T) for minimum-bias and centrality-selected $p + Pb$ collisions, and are compared to the jet rate from the geometric expectation. The total jet yield in minimum-bias events is slightly enhanced above the expectation in a p_T -dependent manner but is consistent with the expectation within uncertainties. The ratios of jet spectra from different centrality selections show a strong modification of jet production at all p_T at forward rapidities and for large p_T at mid-rapidity, which manifests as a suppression of the jet yield in central events and an enhancement in peripheral events. These effects imply that the factorisation between hard and soft processes is violated at an unexpected level in proton–nucleus collisions. Furthermore, the modifications at forward rapidities are found to be a function of the total jet energy only, implying that the violations may have a simple dependence on the hard parton–parton kinematics.

© 2015 CERN for the benefit of the ATLAS Collaboration. Published by Elsevier B.V. This is an open access article under the CC BY license (<http://creativecommons.org/licenses/by/4.0/>). Funded by SCOAP³.

1. Introduction

Proton–lead ($p + Pb$) collisions at the Large Hadron Collider (LHC) provide an excellent opportunity to study hard scattering processes involving a nuclear target [1]. Measurements of jet production in $p + Pb$ collisions provide a valuable benchmark for studies of jet quenching in lead–lead collisions by, for example, constraining the impact of nuclear parton distributions on inclusive jet yields. However, $p + Pb$ collisions also allow the study of possible violations of the QCD factorisation between hard and soft processes which may be enhanced in collisions involving nuclei.

Previous studies in deuteron–gold ($d + Au$) collisions at the Relativistic Heavy Ion Collider (RHIC) observed such violations, manifested in the suppressed production of very forward hadrons with transverse momenta up to 4 GeV [2–4]. Studies of forward dihadron angular correlations at RHIC also showed a much weaker dijet signal in $d + Au$ collisions than in pp collisions [4,5]. These

effects have been attributed to the saturation of the parton distributions in the gold nucleus [6–8], to the modification of the nuclear parton distribution function [9], to the higher-twist contributions to the cross-section enhanced by the forward kinematics of the measurement [10], or to the presence of a large nucleus [11]. The extended kinematic reach of $p + Pb$ measurements at the LHC allows the study of hard scattering processes that produce forward hadrons or jets over a much wider rapidity and transverse momentum range. Such measurements can determine whether the factorisation violations observed at RHIC persist at higher energy and, if so, how the resulting modifications vary as a function of particle or jet momentum and rapidity. The results of such measurements could test the competing descriptions of the RHIC results and, more generally, provide new insight into the physics of hard scattering processes involving a nuclear target.

This paper reports the centrality dependence of inclusive jet production in $p + Pb$ collisions at a nucleon–nucleon centre-of-mass energy $\sqrt{s_{NN}} = 5.02$ TeV. The measurement was performed using a dataset corresponding to an integrated luminosity of 27.8 nb^{-1} recorded in 2013. The $p + Pb$ jet yields were

* E-mail address: atlas.publications@cern.ch.

compared to a nucleon–nucleon reference constructed from a measurement of jet production in pp collisions at a centre-of-mass energy $\sqrt{s} = 2.76$ TeV using a dataset corresponding to an integrated luminosity of 4.0 pb^{-1} also recorded in 2013. Jets were reconstructed from energy deposits measured in the calorimeter using the anti- k_t algorithm with radius parameter $R = 0.4$ [12].

The centrality of $p + \text{Pb}$ collisions was characterised using the total transverse energy measured in the pseudorapidity¹ interval $-4.9 < \eta < -3.2$ in the direction of the lead beam. Whereas in nucleus–nucleus collisions centrality reflects the degree of nuclear overlap between the colliding nuclei, centrality in $p + \text{Pb}$ collisions is sensitive to the multiple interactions between the proton and nucleons in the lead nucleus. Centrality has been successfully used at lower energies in $d + \text{Au}$ collisions at RHIC as an experimental handle on the collision geometry [2,13,14].

A Glauber model [15] was used to determine the average number of nucleon–nucleon collisions, $\langle N_{\text{coll}} \rangle$, and the mean value of the overlap function, $T_{pA}(b) = \int_{-\infty}^{+\infty} \rho(b, z) dz$, where $\rho(b, z)$ is the nucleon density at impact parameter b and longitudinal position z , in each centrality interval. Per-event jet yields, $(1/N_{\text{evt}})(d^2N_{\text{jet}}/dp_T dy^*)$, were measured as a function of jet centre-of-mass rapidity,² y^* , and transverse momentum, p_T , where N_{jet} is the number of jets measured in N_{evt} $p + \text{Pb}$ events analysed. The centrality dependence of the per-event jet yields was evaluated using the nuclear modification factor,

$$R_{p\text{Pb}} \equiv \frac{1}{T_{pA}} \frac{(1/N_{\text{evt}}) d^2N_{\text{jet}}/dp_T dy^*|_{\text{cent}}}{d^2\sigma_{\text{jet}}^{pp}/dp_T dy^*}, \quad (1)$$

for a given centrality selection “cent”, where $d^2\sigma_{\text{jet}}^{pp}/dp_T dy^*$ is determined using the jet cross-section measured in pp collisions at $\sqrt{s} = 2.76$ TeV. The factor $R_{p\text{Pb}}$ quantifies the absolute modification of the jet rate relative to the geometric expectation. In each centrality interval, the geometric expectation is the jet rate that would be produced by an incoherent superposition of the number of nucleon–nucleon collisions corresponding to the mean nuclear thickness in the given class of $p + \text{Pb}$ collisions.

Results are also presented for the central-to-peripheral ratio,

$$R_{\text{CP}} \equiv \frac{1}{R_{\text{coll}}} \frac{(1/N_{\text{evt}}) d^2N_{\text{jet}}/dp_T dy^*|_{\text{cent}}}{(1/N_{\text{evt}}) d^2N_{\text{jet}}/dp_T dy^*|_{\text{peri}}}, \quad (2)$$

where R_{coll} represents the ratio of $\langle N_{\text{coll}} \rangle$ in a given centrality interval to that in the most peripheral interval, $R_{\text{coll}} \equiv \langle N_{\text{coll}}^{\text{cent}} \rangle / \langle N_{\text{coll}}^{\text{peri}} \rangle$. The R_{CP} ratio is sensitive to relative deviations in the jet rate from the geometric expectation between the $p + \text{Pb}$ event centralities. The $R_{p\text{Pb}}$ and R_{CP} measurements are presented as a function of inclusive jet y^* and p_T .

For the 2013 $p + \text{Pb}$ run, the LHC was configured with a 4 TeV proton beam and a 1.57 TeV per-nucleon Pb beam that together produced collisions with $\sqrt{s_{\text{NN}}} = 5.02$ TeV and a rapidity shift of the centre-of-mass frame of 0.465 units relative to the ATLAS rest frame. The run was split into two periods, with the directions of

¹ ATLAS uses a right-handed coordinate system with its origin at the nominal interaction point (IP) in the centre of the detector and the z -axis along the beam pipe. The x -axis points from the IP to the centre of the LHC ring, and the y -axis points upward. Cylindrical coordinates (r, ϕ) are used in the transverse plane, ϕ being the azimuthal angle around the beam pipe. The pseudorapidity is defined in laboratory coordinates in terms of the polar angle θ as $\eta = -\ln \tan(\theta/2)$. During 2013 $p + \text{Pb}$ data-taking, the beam directions were reversed approximately half-way through the running period, but in presenting results the direction of the proton beam is always chosen to point to positive η .

² The jet rapidity y^* is defined as $y^* = 0.5 \ln \frac{E+p_z}{E-p_z}$ where E and p_z are the energy and the component of the momentum along the proton beam direction in the nucleon–nucleon centre-of-mass frame.

the proton and lead beams being reversed at the end of the first period. The first period provided approximately 55% of the integrated luminosity with the Pb beam travelling to positive rapidity and the proton beam to negative rapidity, and the second period provided the remainder with the beams reversed. The analysis in this paper uses the events from both periods of data-taking and y^* is defined so that $y^* > 0$ always refers to the downstream proton direction.

2. Experimental setup

The measurements presented in this paper were performed using the ATLAS inner detector (ID), calorimeters, minimum-bias trigger scintillator (MBTS), and trigger and data acquisition systems [16]. The ID measures charged particles within $|\eta| < 2.5$ using a combination of silicon pixel detectors, silicon microstrip detectors, and a straw-tube transition radiation tracker, all immersed in a 2 T axial magnetic field [17]. The calorimeter system consists of a liquid argon (LAr) electromagnetic (EM) calorimeter covering $|\eta| < 3.2$, a steel/scintillator sampling hadronic calorimeter covering $|\eta| < 1.7$, a LAr hadronic calorimeter covering $1.5 < |\eta| < 3.2$, and two LAr electromagnetic and hadronic forward calorimeters (FCal) covering $3.2 < |\eta| < 4.9$. The EM calorimeters use lead plates as the absorbers and are segmented longitudinally in shower depth into three compartments with an additional presampler layer in front for $|\eta| < 1.8$. The granularity of the EM calorimeter varies with layer and pseudorapidity. The middle sampling layer, which typically has the largest energy deposit in EM showers, has a $\Delta\eta \times \Delta\phi$ granularity of 0.025×0.025 within $|\eta| < 2.5$. The hadronic calorimeter uses steel as the absorber and has three segments longitudinal in shower depth with cell sizes $\Delta\eta \times \Delta\phi = 0.1 \times 0.1$ for $|\eta| < 2.5$ ³ and 0.2×0.2 for $2.5 < |\eta| < 4.9$. The two FCal modules are composed of tungsten and copper absorbers with LAr as the active medium, which together provide ten interaction lengths of material. The MBTS detects charged particles over $2.1 < |\eta| < 3.9$ using two hodoscopes of 16 counters each, positioned at $z = \pm 3.6$ m.

The $p + \text{Pb}$ and pp events used in this analysis were recorded using a combination of minimum-bias (MB) and jet triggers [18]. In $p + \text{Pb}$ data-taking, the MB trigger required hits in at least one counter in each side of the MBTS detector. In pp collisions the MB condition was the presence of hits in the pixel and microstrip detectors reconstructed as a track by the high-level trigger system. Jets were selected using high-level jet triggers implemented with a reconstruction algorithm similar to the procedure applied in the offline analysis. In particular, it used the anti- k_t algorithm with $R = 0.4$, a background subtraction procedure, and a calibration of the jet energy to the full hadronic scale. The high-level jet triggers were seeded from a combination of low-level MB and jet hardware-based triggers. Six jet triggers with transverse energy thresholds ranging from 20 GeV to 75 GeV were used to select jets within $|\eta| < 3.2$ and a separate trigger with a threshold of 15 GeV was used to select jets with $3.2 < |\eta| < 4.9$. The triggers were prescaled in a fashion which varied with time to accommodate the evolution of the luminosity within an LHC fill.

3. Data selection

In the offline analysis, charged-particle tracks were reconstructed in the ID with the same algorithm used in pp collisions [19]. The $p + \text{Pb}$ events used for this analysis were required to have

³ An exception is the third (outermost) sampling layer, which has a segmentation of 0.2×0.1 up to $|\eta| = 1.7$.

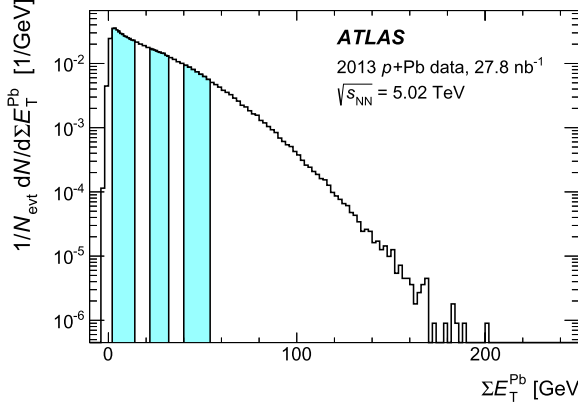


Fig. 1. Distribution of ΣE_T^{Pb} for minimum-bias $p + \text{Pb}$ collisions recorded during the 2013 run, measured in the FCal at $-4.9 < \eta < -3.2$ in the Pb-going direction. The vertical divisions correspond to the six centrality intervals used in this analysis. From right to left, the regions correspond to centrality intervals of 0–10%, 10–20%, 20–30%, 30–40%, 40–60% and 60–90%.

a reconstructed vertex containing at least two associated tracks with $p_T > 0.1$ GeV, at least one hit in each of the two MBTS hodoscopes, and a difference between times measured on the two MBTS sides of less than 10 ns. Events containing multiple $p + \text{Pb}$ collisions (pileup) were suppressed by rejecting events having two or more reconstructed vertices, each associated with reconstructed tracks with a total transverse momentum scalar sum of at least 5 GeV. The fraction of events with one $p + \text{Pb}$ interaction rejected by this requirement was less than 0.1%. Events with a pseudorapidity gap (defined by the absence of clusters in the calorimeter with more than 0.2 GeV of transverse energy) of greater than two units on the Pb-going side of the detector were also removed from the analysis. Such events arise primarily from electromagnetic or diffractive excitation of the proton. After accounting for event selection, the number of $p + \text{Pb}$ events sampled by the highest-luminosity jet trigger (which was unprescaled) was 53 billion. The event selection criteria described here were designed to select a sample of $p + \text{Pb}$ events to which a centrality analysis can be applied and for which meaningful geometric parameters can be determined.

The pp events used in this analysis were required to have a reconstructed vertex, with the same definition as the vertices in $p + \text{Pb}$ events above. No other requirements were applied.

4. Centrality determination

The centrality of the $p + \text{Pb}$ events selected for analysis was characterised by the total transverse energy ΣE_T^{Pb} in the FCal module on the Pb-going side. The ΣE_T^{Pb} distribution for minimum-bias $p + \text{Pb}$ collisions passing the event selection described in Section 3 is presented in Fig. 1. Following standard techniques [20], centrality intervals were defined in terms of percentiles of the ΣE_T^{Pb} distribution after accounting for an estimated inefficiency of $(2 \pm 2)\%$ for inelastic $p + \text{Pb}$ collisions to pass the applied event selection. The following centrality intervals were used in this analysis, in order from the most central to the most peripheral: 0–10%, 10–20%, 20–30%, 30–40%, 40–60%, and 60–90%, with the 60–90% interval serving as the reference in the R_{CP} ratio. Events with a centrality beyond 90% were not used in the analysis, since the uncertainties on the composition of the event sample and in the determination of the geometric quantities are large for these events.

A Glauber Monte Carlo (MC) [15] analysis was used to calculate R_{coll} and T_{pA} for each centrality interval. First, a Glauber MC program [21] was used to simulate the geometry of inelastic

Table 1

Average R_{coll} and T_{pA} values for the centrality intervals used in this analysis along with total systematic uncertainties. The R_{coll} values are with respect to 60–90% events, where $\langle N_{\text{coll}} \rangle = 2.98^{+0.21}_{-0.29}$.

Centrality	R_{coll}	$T_{pA} [\text{mb}^{-1}]$
0–90%	–	$0.107^{+0.005}_{-0.003}$
60–90%	–	$0.043^{+0.003}_{-0.004}$
40–60%	$2.16^{+0.08}_{-0.07}$	$0.092^{+0.004}_{-0.006}$
30–40%	$3.00^{+0.21}_{-0.14}$	$0.126^{+0.003}_{-0.004}$
20–30%	$3.48^{+0.33}_{-0.18}$	$0.148^{+0.004}_{-0.002}$
10–20%	$4.05^{+0.49}_{-0.21}$	$0.172^{+0.007}_{-0.003}$
0–10%	$4.89^{+0.83}_{-0.27}$	$0.208^{+0.019}_{-0.005}$

$p + \text{Pb}$ collisions and calculate the probability distribution of the number of nucleon participants N_{part} , $P(N_{\text{part}})$. The simulations used a Woods–Saxon nuclear density distribution and an inelastic nucleon–nucleon cross-section, σ_{NN} , of 70 ± 5 mb. Separately, PYTHIA 8 [22,23] simulations of 4 TeV on 1.57 TeV pp collisions provided a detector-level ΣE_T^{Pb} distribution for nucleon–nucleon collisions, to be used as input to the Glauber model. This distribution was fit to a gamma distribution.

Then, an extension of the wounded-nucleon (WN) [24] model that included a non-linear dependence of ΣE_T^{Pb} on N_{part} was used to define N_{part} -dependent gamma distributions for ΣE_T^{Pb} , with the constraint that the distributions reduce to the PYTHIA distribution for $N_{\text{part}} = 2$. The non-linear term accounted for the possible variation of the effective FCal acceptance resulting from an N_{part} -dependent backward rapidity shift of the produced soft particles with respect to the nucleon–nucleon frame [25]. The gamma distributions were summed over N_{part} with a $P(N_{\text{part}})$ weighting to produce a hypothetical ΣE_T^{Pb} distribution. That distribution was fit to the measured ΣE_T^{Pb} distribution shown in Fig. 1 with the parameters of the extended WN model allowed to vary freely. The best fit, which contained a significant non-linear term, successfully described the ΣE_T^{Pb} distribution in data over several orders of magnitude. From the results of the fit, the distribution of N_{part} values and the corresponding $\langle N_{\text{part}} \rangle$ were calculated for each centrality interval. The resulting R_{coll} and T_{pA} values and corresponding systematic uncertainties, which are described in Section 8, are shown in Table 1.

5. Monte Carlo simulation

The performance of the jet reconstruction procedure was evaluated using a sample of 36 million events in which simulated $\sqrt{s} = 5.02$ TeV pp hard-scattering events were overlaid with minimum-bias $p + \text{Pb}$ events recorded during the 2013 run. Thus the sample contains an underlying event contribution that is identical in all respects to the data. The simulated events were generated using PYTHIA [22] (version 6.425, AUET2B tune [26], CTEQ6L1 parton distribution functions [27]) and the detector effects were fully simulated using GEANT4 [28,29]. These events were produced for different p_T intervals of the generator-level (“truth”) $R = 0.4$ jets. In total, the generator-level spectrum spans $10 < p_T < 10^3$ GeV. Separate sets of 18 million events each were generated for the two different beam directions to take into account any z -axis asymmetries in the detector. For each beam direction, the four-momenta of the generated particles were longitudinally boosted by a rapidity of ± 0.465 to match the corresponding beam conditions. The events were simulated using detector conditions appropriate to the two periods of the 2013 $p + \text{Pb}$ run and reconstructed using the same algorithms as were applied to the experimental data. A sep-

erate 9-million-event sample of fully simulated 2.76 TeV PYTHIA pp hard scattering events (with the same version, tune and parton distribution function set) was used to evaluate the jet performance in $\sqrt{s} = 2.76$ TeV pp collisions during 2013 data-taking.

6. Jet reconstruction and performance

The jet reconstruction and underlying event subtraction procedures were adapted from those used by ATLAS in $Pb+Pb$ collisions, which are described in detail in Refs. [30,31], and are summarised here along with any substantial differences from the referenced analyses.

An iterative procedure was used to obtain an event-by-event estimate of the underlying event energy density while excluding contributions from jets to that estimate. The modulation of the underlying event energy density to account for potential elliptic flow was not included in this analysis. Jets were reconstructed from the anti- k_t algorithm with $R = 0.4$ applied to calorimeter cells grouped into $\Delta\eta \times \Delta\phi = 0.1 \times 0.1$ towers, with the final jet kinematics calculated from the background-subtracted energy in the cells contained in the jet. The rate of jets reconstructed from the underlying event fluctuations of soft particles was negligible in the kinematic range studied and therefore no attempt to reject them was made. The mean subtracted transverse energy in $p + Pb$ collisions was 2.4 GeV (1.4 GeV) for jets with $|y^*| < 1$ ($y^* > 3$). In pp collisions, this procedure simply subtracts the underlying event pedestal deposited in the calorimeter which can arise, in part, from the presence of additional pp interactions in the same crossing (in-time pileup).

Following the above jet reconstruction, a small correction, typically a few percent, was applied to the transverse momentum of those jets which did not overlap with a region excluded from the background determination and thus were erroneously included in the initial estimate of the underlying event background. Then, the jet energies were corrected to account for the calorimeter energy response using an η - and p_T -dependent multiplicative factor that was derived from the simulations [32]. Following this calibration, a final multiplicative *in situ* calibration was applied to account for differences between the simulated detector response and data. The measured p_T of jets recoiling against objects with an independently calibrated energy scale – such as Z bosons, photons, or jets in a different region of the detector – was investigated. The *in situ* calibration, which typically differed from unity by a few percent, was derived by comparing this p_T balance in pp data with that in simulations in a fashion similar to that used previously within ATLAS [33].

The jet reconstruction performance was evaluated in the simulated samples by applying the same subtraction and reconstruction procedure as was applied to data. The resulting reconstructed jets with transverse momentum p_T^{reco} were compared with their corresponding generator jets, which were produced by applying the anti- k_t algorithm to the final-state particles produced by PYTHIA, excluding muons and neutrinos. Each generator jet was matched to a reconstructed jet, and the p_T difference between the two jets was studied as a function of the generator jet transverse momentum, p_T^{gen} , and generator jet rapidity y^* , and in the six $p + Pb$ event centrality intervals.

The reconstruction efficiency for jets having $p_T^{\text{gen}} > 25$ GeV was found to be greater than 99%. The performance was quantified by the means and standard deviations of the $\Delta p_T/p_T$ ($= p_T^{\text{reco}}/p_T^{\text{gen}} - 1$) distributions, referred to as the jet energy scale closure and jet energy resolution respectively. The closure in $p + Pb$ events was less than 2% for $p_T^{\text{gen}} > 25$ GeV jets and was better than 1% for $p_T^{\text{gen}} > 100$ GeV jets. At low p_T^{gen} , the energy scale closure and resolution exhibited a weak $p + Pb$ centrality dependence,

with differences in the closure of up to 1% and differences in the resolution of up to 2% in the most central 0–10% events relative to the 60–90% peripheral events. At high jet p_T , the response was centrality independent within sensitivity. In pp events, the closure was less than 1% in the entire kinematic range studied.

In order to quantify the degree of p_T -bin migration introduced by the detector response and reconstruction procedure, response matrices were populated by recording the p_T values of each generator-reconstructed jet pair. Separate matrices were constructed for each y^* interval and $p + Pb$ centrality interval used in the analysis. The p_T bins used were chosen to increase with p_T such that the width of each bin was ≈ 0.25 of the bin low edge. Using this binning, the proportion of jets with reconstructed p_T in the same bin as their truth p_T monotonically increased with truth p_T and was 50–70%.

7. Data analysis

A combination of minimum-bias and jet triggered $p + Pb$ events were selected for analysis as described in Section 2. The sampled luminosity (defined as the luminosity divided by the mean luminosity-weighted prescale) of the jet triggers increased with increasing p_T threshold. Offline jets were selected for the analysis by requiring a match to an online jet trigger. The efficiency of the various triggers was determined with respect to the minimum-bias trigger and to lower threshold jet triggers. For simplicity, each p_T bin used jets selected by only one jet trigger. In a given p_T bin, jets were selected by the highest-threshold jet trigger for which the efficiency was determined to be greater than 99% in the bin. No additional corrections for the trigger efficiency were applied.

The double-differential per-event jet yields in $p + Pb$ collisions were constructed via

$$\frac{1}{N_{\text{evt}}} \frac{d^2 N_{\text{jet}}}{dp_T dy^*} = \frac{1}{N_{\text{evt}}} \frac{N_{\text{jet}}}{\Delta p_T \Delta y^*}, \quad (3)$$

where N_{evt} is the total (unprescaled) number of MB $p + Pb$ events sampled, $N_{\text{jet}}^{\text{jet}}$ is the yield of jets corrected for all detector effects and the instantaneous trigger prescale during data-taking, and Δp_T and Δy^* are the widths of the p_T and y^* bins. The centrality-dependent yields were constructed by restricting N_{evt} and $N_{\text{jet}}^{\text{jet}}$ to come from $p + Pb$ events within a given centrality interval. The double-differential cross-section in pp collisions was constructed via

$$\frac{d^2 \sigma}{dp_T dy^*} = \frac{1}{L_{\text{int}}} \frac{N_{\text{jet}}^{\text{jet}}}{\Delta p_T \Delta y^*}, \quad (4)$$

where L_{int} is the total integrated luminosity of the jet trigger used in the given p_T bin. The p_T binning in the pp cross-section was chosen such that the $x_T = 2p_T/\sqrt{s}$ binning between the $p + Pb$ and pp datasets is the same.

Both the per-event yields in $p + Pb$ collisions and the cross-section in pp collisions were restricted to the p_T range where the MC studies described in Section 6 show that the efficiency for a truth jet to remain in the same p_T bin is $\geq 50\%$. This p_T range was rapidity dependent, with the lowest p_T bin edge used ranging from 50 GeV in the most backward rapidity intervals studied to 25 GeV in the most forward intervals.

The measured $p + Pb$ and pp yields were corrected for jet energy resolution and residual distortions of the jet energy scale which result in p_T -bin migration. For each rapidity interval, the yield was corrected by the use of p_T -dependent (and, in the $p + Pb$ case, centrality-dependent) bin-by-bin correction factors $C(p_T, y^*)$ obtained from the ratio of the reconstructed to the truth jet p_T distributions for jets originating in a true y^* bin, according to

$$C(p_T, y^*) = \frac{N_{\text{truth}}^{\text{jet}}(p_T, y^*)}{N_{\text{reco}}^{\text{jet}}(p_T, y^*)}, \quad (5)$$

where $N_{\text{truth}}^{\text{jet}}$ ($N_{\text{reco}}^{\text{jet}}$) is the number of truth jets in the given p_T^{truth} (p_T^{reco}) bin in the corresponding MC samples.

Since the determination of the correction factors $C(p_T, y^*)$ is sensitive to the shape of the jet spectrum in the MC sample, the response matrices used to generate them were reweighted to provide a better match between the reconstructed distributions in data and simulated events. The spectrum of generator jets was weighted jet-by-jet by the ratio of the reconstructed spectrum in data to that in simulation. This ratio was found to be approximately linear in the logarithm of reconstructed p_T . A separate reweighting was performed for the $p + \text{Pb}$ jet yield in each centrality interval, resulting in changes of $\leq 10\%$ from the original correction factors before reweighting. The resulting corrections to the $p + \text{Pb}$ and pp yields were at most 30%, and were typically $\leq 10\%$ for jets with $p_T > 100 \text{ GeV}$. These corrections were applied to the detector-level yield $N_{\text{reco}}^{\text{jet}}$ to give the particle-level yield via

$$N^{\text{jet}} = C(p_T, y^*) N_{\text{reco}}^{\text{jet}}. \quad (6)$$

A $\sqrt{s} = 5.02 \text{ TeV}$ pp reference jet cross-section was constructed through the use of the corrected 2.76 TeV pp cross-section and a previous ATLAS measurement of the x_T -scaling between the inclusive jet cross-sections at $\sqrt{s} = 2.76 \text{ TeV}$ (measured using 0.20 pb^{-1} of data collected in 2011) and 7 TeV (measured using 37 pb^{-1} of data collected in 2010) [34]. In this previous analysis, the \sqrt{s} -scaled ratio ρ of the 2.76 TeV cross-section to that at 7 TeV was evaluated at fixed x_T ,

$$\rho(x_T; y^*) = \left(\frac{2.76 \text{ TeV}}{7 \text{ TeV}} \right)^3 \frac{d^2\sigma^{2.76 \text{ TeV}}/dp_T dy^*}{d^2\sigma^{7 \text{ TeV}}/dp_T dy^*}, \quad (7)$$

where $d^2\sigma/\sqrt{s}/dp_T dy^*$ is the pp jet cross-section at the given centre-of-mass energy \sqrt{s} , and the numerator and denominator are each evaluated at the same x_T (but different $p_T = x_T \sqrt{s}/2$). Equation (7) can be rearranged to define the cross-section at $\sqrt{s} = 7 \text{ TeV}$ in terms of that at 2.76 TeV times a multiplicative factor and divided by ρ .

The $\sqrt{s} = 5.02 \text{ TeV}$ pp cross-section at each p_T and y^* value was constructed by scaling the corrected $\sqrt{s} = 2.76 \text{ TeV}$ pp cross-section measured at the equivalent x_T according to

$$\frac{d^2\sigma^{5.02 \text{ TeV}}}{dp_T dy^*} = \rho(x_T; y^*)^{-0.643} \left(\frac{2.76 \text{ TeV}}{5.02 \text{ TeV}} \right)^3 \frac{d^2\sigma^{2.76 \text{ TeV}}}{dp_T dy^*}, \quad (8)$$

where the power $-\ln(2.76/5.02)/\ln(2.76/7) \approx -0.643$ interpolates between 2.76 TeV and 7 TeV to 5.02 TeV using a power-law collision energy dependence at each p_T and y^* . Since the jet energy scale and x_T -interpolation uncertainties are large for the pp data at large rapidities ($|y^*| > 2.8$), a $\sqrt{s} = 5.02 \text{ TeV}$ reference is not constructed in that rapidity region.

The pp jet cross-section at $\sqrt{s} = 2.76 \text{ TeV}$ measured with the 2013 data was found to agree with the previous ATLAS measurement of the same quantity [34] within the systematic uncertainties.

8. Systematic uncertainties

The R_{CP} and $R_{p\text{Pb}}$ measurements are subject to systematic uncertainties arising from a number of sources: the jet energy scale and resolution, differences in the spectral shape between data and simulation affecting the bin-by-bin correction factors, residual inefficiency in the trigger selection, and the estimates of the geometric quantities R_{coll} (in R_{CP}) and T_{pA} (in $R_{p\text{Pb}}$). In addition

to these sources of uncertainty, which are common to the R_{CP} and $R_{p\text{Pb}}$ measurements, $R_{p\text{Pb}}$ is also subject to uncertainties from the x_T -interpolation of the $\sqrt{s} = 2.76 \text{ TeV}$ pp cross-section to the $\sqrt{s} = 5.02 \text{ TeV}$ centre-of-mass energy and from the integrated luminosity of the pp dataset.

Uncertainties in the jet energy scale and resolution influence the correction of the $p + \text{Pb}$ and pp jet spectra. The uncertainty in the scale was taken from studies of the *in situ* calorimeter response and systematic variations of the jet response in simulation [32], as well as studies of the relative energy scale difference between the jet reconstruction procedure in heavy-ion collisions and the procedure used by ATLAS for inclusive jet measurements in 2.76 TeV and 7 TeV pp collisions [34,35]. The total energy scale uncertainty in the measured p_T range was $\lesssim 4\%$ for jets in $|y^*| < 2.8$, and $\lesssim 7\%$ for jets in $|y^*| > 2.8$. The sensitivity of the results to the uncertainty in the energy scale was evaluated separately for ten distinct sources of uncertainty. Each source was treated as fully uncorrelated with any other source, but fully correlated with itself in p_T , η , and \sqrt{s} . The uncertainty in the resolution was taken from *in situ* studies of the dijet energy balance [36]. The resolution uncertainty was generally $< 10\%$, except for low- p_T jets where it was $< 20\%$. The effects on the R_{CP} and $R_{p\text{Pb}}$ measurements were evaluated through an additional smearing of the energy of reconstructed jets in the simulation such that the resolution uncertainty was added to the original resolution in quadrature.

The resulting systematic uncertainties on R_{CP} (δR_{CP}) and $R_{p\text{Pb}}$ ($\delta R_{p\text{Pb}}$) were evaluated by producing new response matrices in accordance with each source of the energy scale uncertainty and the resolution uncertainty, generating new correction factors, and calculating the new R_{CP} and $R_{p\text{Pb}}$ results. Each energy scale and resolution variation was applied to all rapidity bins and to both the $p + \text{Pb}$ and pp response matrices simultaneously. The uncertainty on R_{CP} and $R_{p\text{Pb}}$ from the total energy scale uncertainty was determined by adding the effects of the ten energy scale uncertainty sources in quadrature. Since the correction factors for the $p + \text{Pb}$ spectra in different centrality intervals were affected to a similar degree by variations in the energy scale and resolution, the effects tended to cancel in the R_{CP} ratio, and the resulting δR_{CP} were small. The resulting $\delta R_{p\text{Pb}}$ values were somewhat larger than the δR_{CP} values due to the relative centre-of-mass shift between the $p + \text{Pb}$ and pp collision systems. The centrality dependence of the energy scale and resolution uncertainties in $p + \text{Pb}$ events was negligible.

To achieve better correspondence with the data, the simulated jet spectrum was reweighted to match the spectral shape in data before deriving the bin-by-bin correction factors as described above. To determine the sensitivity of the results to this reweighting procedure, the slope of the fit to the ratio of the detector-level spectrum in data to that in simulation was varied by the fit uncertainty, and the correction factors were recomputed with this alternative weighting. The resulting $\delta R_{p\text{Pb}}$ and δR_{CP} from the nominal values were included in the total systematic uncertainty.

As the jet triggers used for the data selection were evaluated to have greater than 99% efficiency in the p_T regions where they are used to select jets, an uncertainty of 1% was chosen for the centrality selected $p + \text{Pb}$ yields and the pp cross-section in the range $20 < p_T < 125 \text{ GeV}$. This uncertainty was taken to be uncorrelated between the centrality-selected $p + \text{Pb}$ yields and the pp cross-section, resulting in a 1.4% uncertainty on the R_{CP} and $R_{p\text{Pb}}$ measurements.

The geometric quantities R_{coll} and T_{pA} and their uncertainties are listed in Table 1. These uncertainties arise from uncertainties in the geometric modelling of $p + \text{Pb}$ collisions and in modelling the N_{part} dependence of the forward particle production measured by ΣE_T^{Pb} . In general, the uncertainties were asymmetric.

Uncertainties in R_{coll} were largest for the ratio of the most central to the most peripheral interval (0–10%/60–90%), where they were +17/−6%, and smallest in the 40–60%/60–90% ratio, where they were +4/−3%. Uncertainties in T_{pA} were largest in the most central (0–10%) and most peripheral (60–90%) centrality intervals, where the upper or lower uncertainty was as high as 10%, and smaller for intervals in the middle of the $p + \text{Pb}$ centrality range, where they reached a minimum of +3/−2% for the 20–30% interval.

The x_{T} -interpolation of the $\sqrt{s} = 2.76$ TeV pp jet cross-section to 5.02 TeV is sensitive to uncertainties in $\rho(x_{\text{T}}, y^*)$, the \sqrt{s} -scaled ratio of jet spectra at 2.76 and 7 TeV. Following Eq. (8), the uncertainty in the interpolated pp cross-section ($\delta\sigma^{5.02 \text{ TeV}}$) at fixed x_{T} is related to the uncertainty in ρ ($\delta\rho$) via $(\delta\sigma^{5.02 \text{ TeV}}/\sigma^{5.02 \text{ TeV}}) = 0.643(\delta\rho/\rho)$, where $\delta\rho$ was taken from Ref. [34]. The values of $\delta\rho$ ranged from 5% to 23% in the region of the measurement and were generally larger at lower x_{T} and at larger rapidities.

The integrated luminosity for the 2013 pp dataset was determined by measuring the interaction rate with several ATLAS sub-detectors. The absolute calibration was derived from three van der Meer scans [37] performed during the pp data-taking in 2013 in a fashion similar to that used previously within ATLAS [38] for pp data-taking at higher energies. The systematic uncertainty on the integrated luminosity was estimated to be 3.1%.

The uncertainties from the jet energy scale, jet energy resolution, reweighting and x_{T} -interpolation are p_{T} and y^* dependent, while the uncertainties from the trigger, luminosity, and geometric factors are not. The total systematic uncertainty on the R_{pPb} measurement ranges from 7% at mid-rapidity and high p_{T} to 18% at forward rapidities and low p_{T} . In most p_{T} and rapidity bins, the dominant systematic uncertainty on R_{pPb} is from the x_{T} -interpolation. The p_{T} - and y^* -dependent systematic uncertainties on R_{CP} are small. Near mid-rapidity or at high p_{T} , they are 2%, rising to approximately 12% at low p_{T} in forward rapidities. Thus, in most of the kinematic region studied, the dominant uncertainty on R_{CP} is from the geometric factors R_{coll} .

9. Results

Fig. 2 presents the fully corrected per-event jet yield as a function of p_{T} in 0–90% $p + \text{Pb}$ collisions, for each of the jet centre-of-mass rapidity ranges used in this analysis. At mid-rapidity, the yields span over eight orders of magnitude.

The jet nuclear modification factor R_{pPb} for 0–90% $p + \text{Pb}$ events is presented in **Fig. 3** in the eight rapidity bins for which the pp reference was constructed. At most rapidities studied, the R_{pPb} values show a slight ($\approx 10\%$) enhancement above one, although many bins are consistent with unity within the systematic uncertainties. At mid-rapidity, the R_{pPb} values reach a maximum near 100 GeV. No large modification of the total yield of jets relative to the geometric expectation (under which $R_{\text{pPb}} = 1$) is observed. The data in **Fig. 3** are compared to a next-to-leading order perturbative QCD calculation of R_{pPb} with the EPS09 parameterisation of nuclear parton distribution functions [9], using CT10 [39] for the free proton parton distribution functions and following the procedure for calculating jet production rates in $p + \text{Pb}$ collisions described in Refs. [1,40]. The data are slightly higher than the calculation, but generally compatible with it within systematic uncertainties.

The central-to-peripheral ratio R_{CP} for jets in $p + \text{Pb}$ collisions is summarised in **Fig. 4**, where the R_{CP} values for three centrality intervals are shown in all rapidity ranges studied. The R_{CP} ratio shows a strong variation with centrality relative to the geometric expectation, under which $R_{\text{CP}} = 1$. The jet R_{CP} for 0–10%/60–90% events is smaller than one at all rapidities for jet $p_{\text{T}} > 100$ GeV

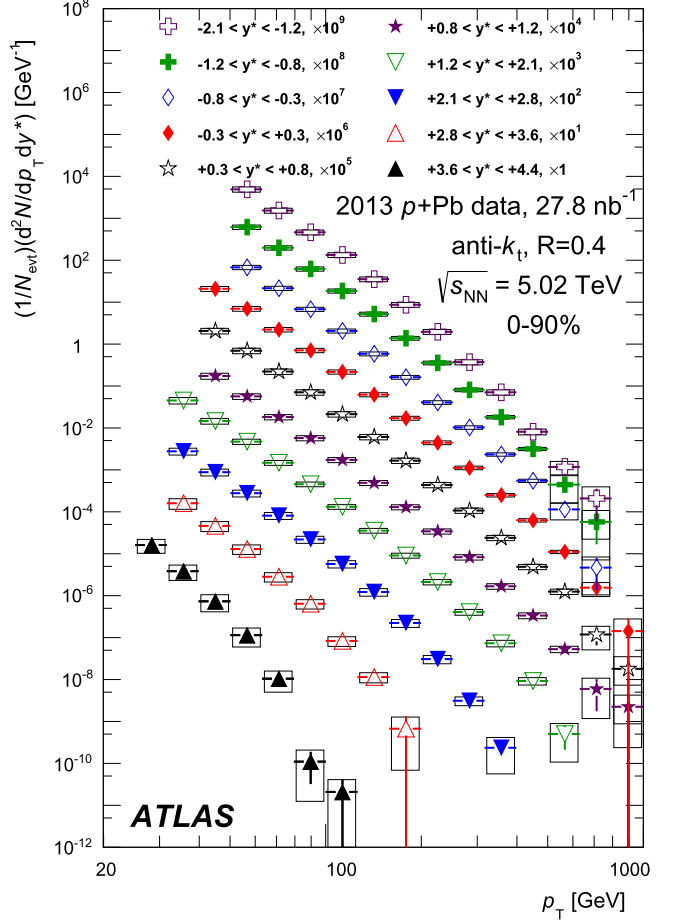


Fig. 2. Inclusive double-differential per-event jet yield in 0–90% $p + \text{Pb}$ collisions as a function of jet p_{T} in different y^* bins. The yields are corrected for all detector effects. Vertical error bars represent the statistical uncertainty while the boxes represent the systematic uncertainties.

and at all p_{T} at sufficiently forward (proton-going, $y^* > 0$) rapidities. Near mid-rapidity, the 40–60%/60–90% R_{CP} values are consistent with unity up to 100–200 GeV, but indicate a small suppression at higher p_{T} . In all rapidity intervals studied, R_{CP} decreases with increasing p_{T} and in increasingly more central collisions. Furthermore, at fixed p_{T} , R_{CP} decreases systematically at more forward rapidities. At the highest p_{T} in the most forward rapidity bin, the 0–10%/60–90% R_{CP} value is ≈ 0.2 . In the backward rapidity direction (lead-going, $y^* < 0$), R_{CP} is found to be enhanced by 10–20% for low- p_{T} jets.

Fig. 5 summarises the jet R_{pPb} in central, mid-central and peripheral events in all rapidity intervals studied. The patterns observed in the centrality-dependent R_{pPb} values are a consequence of the near-geometric scaling of the minimum-bias R_{pPb} values along with the strong modifications of the central-to-peripheral ratio R_{CP} . At sufficiently high p_{T} , R_{pPb} in central events is found to be suppressed ($R_{\text{pPb}} < 1$) and in peripheral events to be enhanced ($R_{\text{pPb}} > 1$). Generally, these respective deviations from the geometric expectation (under which $R_{\text{pPb}} = 1$ for all centrality intervals) increase with p_{T} and, at fixed p_{T} , increase as the rapidity becomes more forward. Thus, the large effects in R_{CP} are consistent with a combination of modifications that have opposite sign in the centrality-dependent R_{pPb} values but have little effect on the centrality-inclusive (0–90%) R_{pPb} values. At backward-going rapidities ($y^* < 0$) the R_{pPb} value for low- p_{T} jets in all centrality intervals is consistent with unity within the uncertainties.

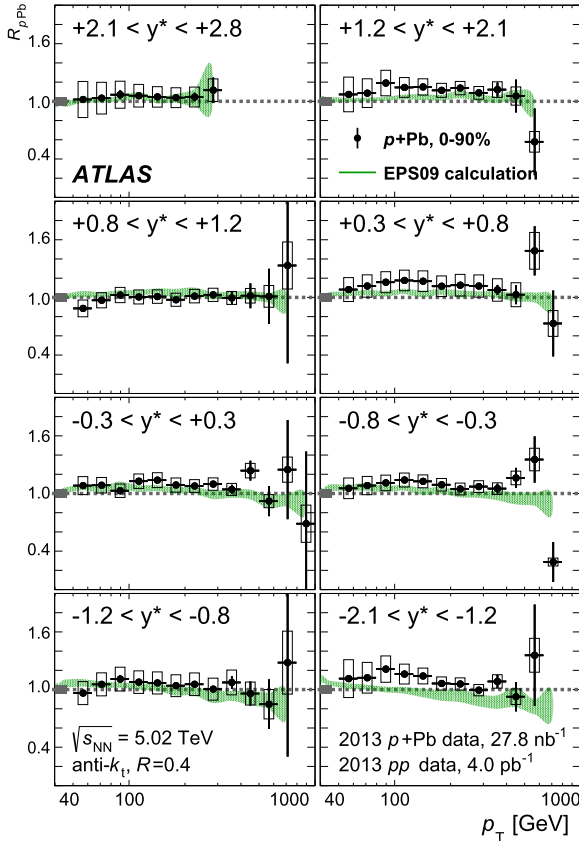


Fig. 3. Measured $R_{p\text{Pb}}$ values for $R = 0.4$ jets in 0–90% $p + \text{Pb}$ collisions. Each panel shows the jet $R_{p\text{Pb}}$ in a different rapidity range. Vertical error bars represent the statistical uncertainty while the boxes represent the systematic uncertainties on the jet yields. The shaded box at the left edge of the $R_{p\text{Pb}} = 1$ horizontal line indicates the systematic uncertainty on T_{pA} and the pp luminosity in quadrature. The shaded band represents a calculation using the EPS09 nuclear parton distribution function set.

Given the observed suppression pattern as a function of jet rapidity, in which the suppression in R_{CP} at fixed p_T systematically increases at more forward-going rapidities, it is natural to ask if it is possible to find a single relationship between the R_{CP} values in the different rapidity intervals which is a function of jet kinematics alone. To test this, the R_{CP} values in each rapidity bin were plotted against the quantity $p_T \times \cosh(\langle y^* \rangle) \approx E$, where $\langle y^* \rangle$ is the centre of the rapidity bin and E is the total energy of the jet. In relativistic kinematics, the total energy of a particle is given by $E = m_T \cosh(y^*)$, where the transverse mass $m_T = \sqrt{m^2 + p_T^2}$. In the kinematic range studied, the mass of the typical jet is sufficiently small relative to its transverse momentum that approximating the transverse mass, m_T , with the p_T is reasonable. The 0–10%/60–90% R_{CP} versus $p_T \times \cosh(\langle y^* \rangle)$ is shown for all ten rapidity ranges in Fig. 6. When plotted against this variable, the R_{CP} values in each of the five forward-going rapidities ($y^* > +0.8$) fall along the same curve, which is approximately linear in the logarithm of E . This trend is also observed in the two most forward of the remaining rapidity intervals ($-0.3 < y^* < +0.8$), but the R_{CP} values at backward rapidities ($y^* < -0.3$) do not follow this trend. This pattern is also observed in other centrality intervals, albeit with a different slope in $\ln(E)$ for each centrality interval.

These patterns suggest that the observed modifications may depend on the initial parton kinematics, such as the longitudinal momentum fraction of the parton originating in the proton, x_p . In particular, a dependence on x_p would explain why the data fol-

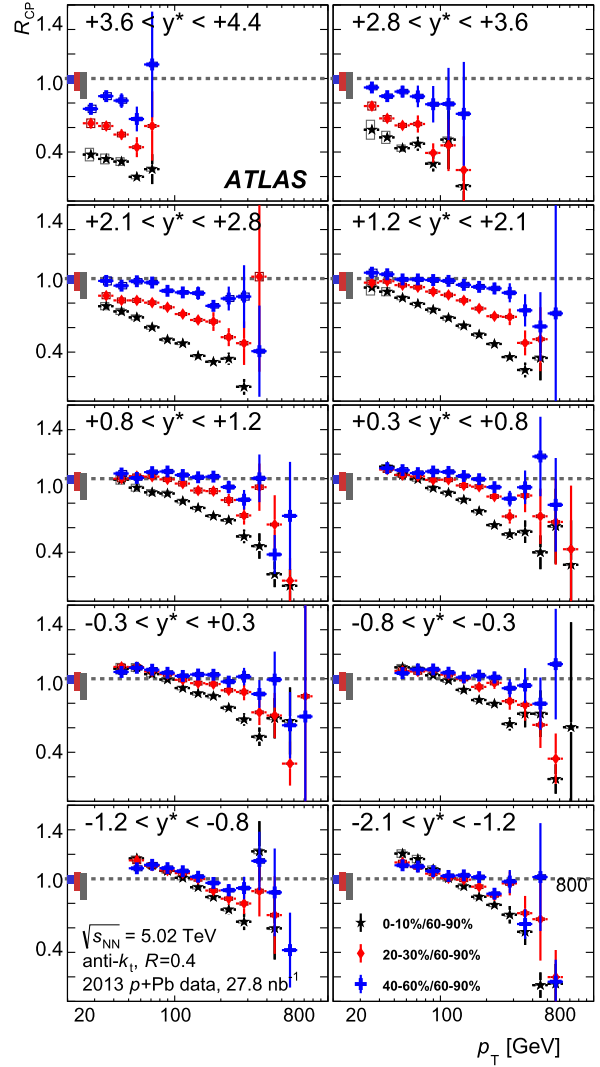


Fig. 4. Measured R_{CP} values for $R = 0.4$ jets in $p + \text{Pb}$ collisions in central (stars), mid-central (diamonds) and mid-peripheral (crosses) events. Each panel shows the jet R_{CP} in a different rapidity range. Vertical error bars represent the statistical uncertainty while the boxes represent the systematic uncertainties on the jet yields. The shaded boxes at the left edge of the $R_{\text{CP}} = 1$ horizontal line indicate the systematic uncertainty on R_{coll} for (from left to right) peripheral, mid-central and central events.

low a consistent trend vs. $p_T \times \cosh(\langle y^* \rangle)$ at forward rapidities (where jet production at a given jet energy E is dominated by $x_p \sim E/(\sqrt{s}/2)$ partons in the proton) but do not do so at backward rapidities (where the longitudinal momentum fraction of the parton originating in the lead nucleus, x_{pb} , as well as x_p are both needed to relate the jet and parton kinematics).

By analogy with Fig. 6 where the R_{CP} values are plotted versus $p_T \times \cosh(\langle y^* \rangle)$, the $R_{p\text{Pb}}$ values in the four most forward-going bins studied are plotted against this variable in Fig. 7. The $R_{p\text{Pb}}$ values in central and peripheral events are shown separately. Although the systematic uncertainties are larger on $R_{p\text{Pb}}$ than on R_{CP} , the observed behaviour for jets with $p_T > 150$ GeV is consistent with the nuclear modifications depending only on the approximate total jet energy $p_T \times \cosh(\langle y^* \rangle)$. In central (peripheral) events, the $R_{p\text{Pb}}$ values at forward rapidities are consistent with a rapidity-independent decreasing (increasing) function of $p_T \times \cosh(\langle y^* \rangle)$. Thus, the single trend in R_{CP} versus $p_T \times \cosh(\langle y^* \rangle)$ at forward rapidities appears to arise from opposite trends in the central and peripheral $R_{p\text{Pb}}$, both a single function of $p_T \times \cosh(\langle y^* \rangle)$.

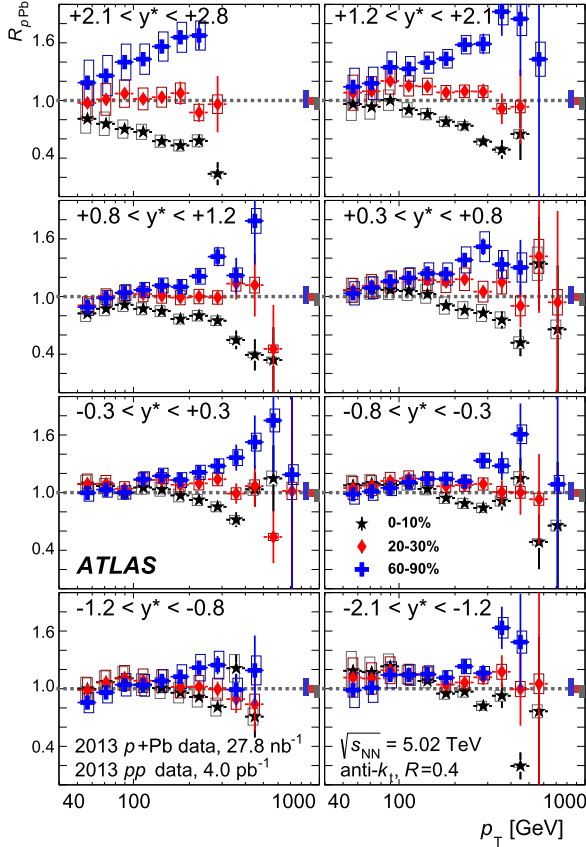


Fig. 5. Measured $R_{p\text{Pb}}$ values for $R = 0.4$ jets in $p + \text{Pb}$ collisions in central (stars), mid-central (diamonds) and peripheral (crosses) events. Each panel shows the jet $R_{p\text{Pb}}$ in a different rapidity range. Vertical error bars represent the statistical uncertainty while the boxes represent the systematic uncertainties on the jet yields. The shaded boxes at the right edge of the $R_{p\text{Pb}} = 1$ horizontal line indicate the systematic uncertainties on T_{pA} and the pp luminosity added in quadrature for (from left to right) peripheral, mid-central and central events.

The results presented here use the standard Glauber model with fixed σ_{NN} to estimate the geometric quantities. The impact of geometric models which incorporate event-by-event changes in the configuration of the proton wavefunction [41] has also been studied. Using the so called Glauber–Gribov Colour Fluctuation model to determine the geometric parameters amplifies the effects seen with the Glauber model. In this model, the suppression in central events and the enhancement in peripheral events would be increased.

10. Conclusions

This paper presents the results of a measurement of the centrality dependence of jet production in $p + \text{Pb}$ collisions at $\sqrt{s_{\text{NN}}} = 5.02$ TeV over a wide kinematic range. The data were collected with the ATLAS detector at the LHC and correspond to 27.8 nb^{-1} of integrated luminosity. The centrality of $p + \text{Pb}$ collisions was characterised using the total transverse energy measured in the forward calorimeter on the Pb-going side covering the interval $-4.9 < \eta < -3.2$. The average number of nucleon–nucleon collisions and the mean nuclear thickness factor were evaluated for each centrality interval using a Glauber Monte Carlo analysis.

Results are presented for the nuclear modification factor $R_{p\text{Pb}}$ with respect to a measurement of the inclusive jet cross-section in $\sqrt{s} = 2.76$ TeV pp collisions corresponding to 4.0 pb^{-1} of integrated luminosity. The pp cross-section was x_T -interpolated to 5.02 TeV using previous ATLAS measurements of inclusive jet pro-

duction at 2.76 and 7 TeV. Results are also shown for the central-to-peripheral ratio R_{CP} . The centrality-inclusive $R_{p\text{Pb}}$ results for 0–90% collisions indicate only a modest enhancement over the geometric expectation. This enhancement has a weak p_T and rapidity dependence and is generally consistent with predictions from the modification of the parton distribution functions in the nucleus, which is small in the kinematic region probed by this measurement.

The results of the R_{CP} measurement indicate a strong centrality-dependent reduction in the yield of jets in central collisions relative to that in peripheral collisions, after accounting for the effects of the collision geometries. In addition, the reduction becomes more pronounced with increasing jet p_T and at more forward (downstream proton) rapidities. These two results are reconciled by the centrality-dependent $R_{p\text{Pb}}$ results, which show a suppression in central collisions and enhancement in peripheral collisions, a pattern which is systematic in p_T and y^* .

The R_{CP} and $R_{p\text{Pb}}$ measurements at forward rapidities are also reported as a function of $p_T \times \cosh(y^*)$, the approximate total jet energy. When plotted this way, the results from different rapidity intervals follow a similar trend. This suggests that the mechanism responsible for the observed effects may depend only on the total jet energy or, more generally, on the underlying parton–parton kinematics such as the fractional longitudinal momentum of the parton originating in the proton.

If the relationship between the centrality intervals and proton–lead collision impact parameter determined by the geometric models is correct, these results imply large, impact parameter-dependent changes in the number of partons available for hard scattering. However, they may also be the result of a correlation between the kinematics of the scattering and the soft interactions resulting in particle production at backward (Pb-going) rapidities [42,43].

Recently, the effects observed here have been hypothesised as arising from a suppression of the soft particle multiplicity in collisions producing high energy jets [44]. Independently, it has also been argued that proton configurations containing a large- x parton interact with nucleons in the nucleus with a reduced cross-section, resulting in the observed modifications [45]. In any case the presence of such correlations would challenge the usual factorisation-based framework for describing hard scattering processes in collisions involving nuclei.

Acknowledgements

We thank CERN for the very successful operation of the LHC, as well as the support staff from our institutions without whom ATLAS could not be operated efficiently.

We acknowledge the support of ANPCyT, Argentina; YerPhI, Armenia; ARC, Australia; BMWFW and FWF, Austria; ANAS, Azerbaijan; SSTC, Belarus; CNPq and FAPESP, Brazil; NSERC, NRC and CFI, Canada; CERN; CONICYT, Chile; CAS, MOST and NSFC, China; COLCIENCIAS, Colombia; MSMT CR, MPO CR and VSC CR, Czech Republic; DNRF, DNSRC and Lundbeck Foundation, Denmark; EPLANET, ERC and NSRF, European Union; IN2P3-CNRS, CEA-DSM/IRFU, France; GNSF, Georgia; BMBF, DFG, HGF, MPG and AvH Foundation, Germany; GSRT and NSRF, Greece; ISF, MINERVA, GIF, I-CORE and Benoziyo Center, Israel; INFN, Italy; MEXT and JSPS, Japan; CNRST, Morocco; FOM and NWO, Netherlands; BRF and RCN, Norway; MNiSW and NCN, Poland; GRICES and FCT, Portugal; MNE/IFA, Romania; MES of Russia and ROSATOM, Russian Federation; JINR; MSTD, Serbia; MSSR, Slovakia; ARRS and MIZŠ, Slovenia; DST/NRF, South Africa; MINECO, Spain; SRC and Wallenberg Foundation, Sweden; SER, SNSF and Cantons of Bern and Geneva, Switzerland; NSC, Taiwan; TAEK, Turkey; STFC, the

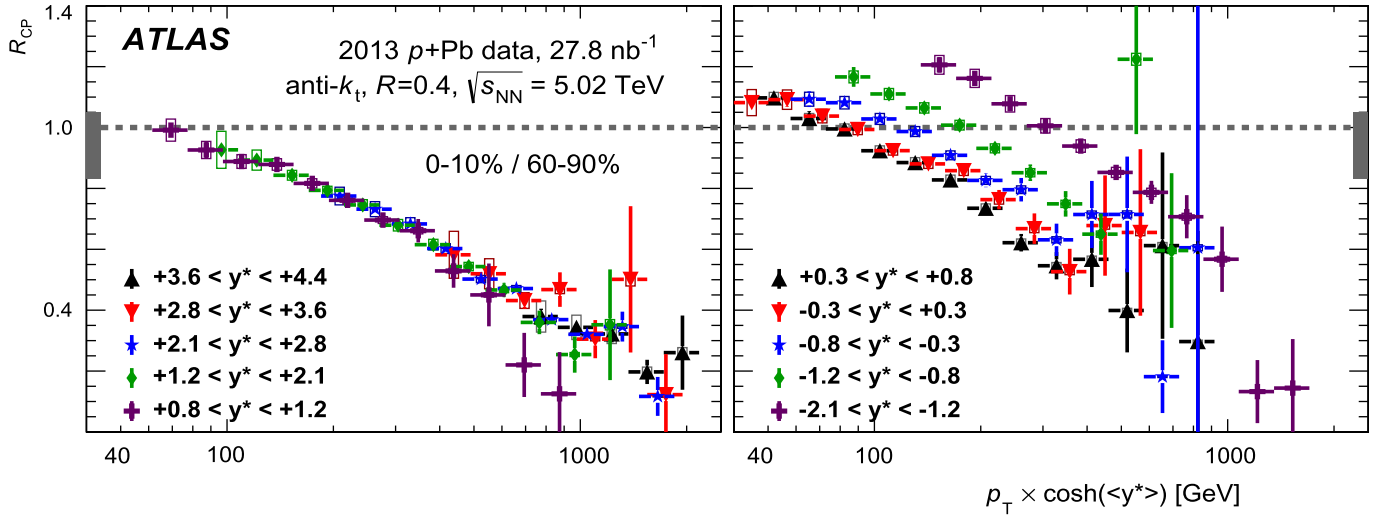


Fig. 6. Measured R_{CP} values for $R = 0.4$ jets in 0–10% $p + Pb$ collisions. The panel on the left shows the five rapidity ranges that are the most forward-going, while the panel on the right shows the remaining five. The R_{CP} values at each rapidity are plotted as a function of $p_T \times \cosh(\langle y^* \rangle)$, where $\langle y^* \rangle$ is the midpoint of the rapidity bin. Vertical error bars represent the statistical uncertainty while the boxes represent the systematic uncertainties on the jet yields. The shaded box at the left edge (in the left panel) and right edge (in the right panel) of the $R_{CP} = 1$ horizontal line indicates the systematic uncertainty on R_{coll} .

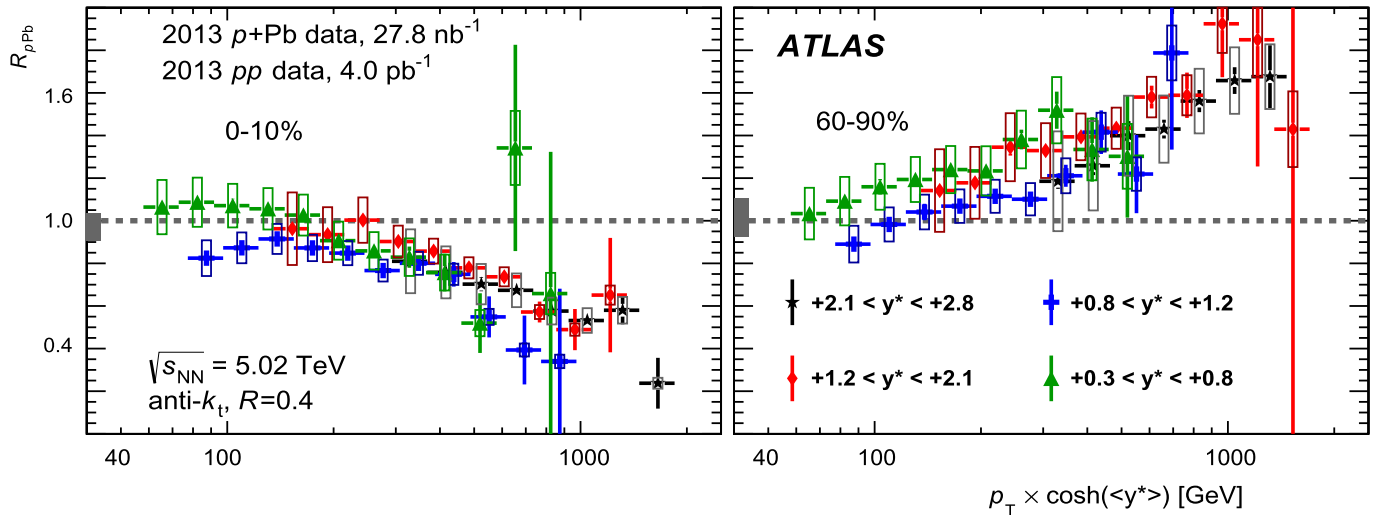


Fig. 7. Measured R_{ppb} values for $R = 0.4$ jets in $p + Pb$ collisions displayed for multiple rapidity ranges, showing 0–10% events in the left panel and 60–90% events in the right panel. The R_{ppb} at each rapidity is plotted as a function of $p_T \times \cosh(\langle y^* \rangle)$, where $\langle y^* \rangle$ is the midpoint of the rapidity bin. Vertical error bars represent the statistical uncertainty while the boxes represent the systematic uncertainties on the jet yields. The shaded box at the left edge of the $R_{ppb} = 1$ horizontal line indicates the systematic uncertainties on T_{pA} and the pp luminosity added in quadrature.

Royal Society and Leverhulme Trust, United Kingdom; DOE and NSF, United States of America.

The crucial computing support from all WLCG partners is acknowledged gratefully, in particular from CERN and the ATLAS Tier-1 facilities at TRIUMF (Canada), NDGF (Denmark, Norway, Sweden), CC-IN2P3 (France), KIT/GridKA (Germany), INFN-CNAF (Italy), NL-T1 (Netherlands), PIC (Spain), ASGC (Taiwan), RAL (UK) and BNL (USA) and in the Tier-2 facilities worldwide.

References

- [1] C. Salgado, et al., J. Phys. G 39 (2012) 015010, arXiv:1105.3919.
- [2] I. Arsene, et al., Phys. Rev. Lett. 93 (2004) 242303, arXiv:nucl-ex/0403005.
- [3] S.S. Adler, et al., Phys. Rev. Lett. 94 (2005) 082302, arXiv:nucl-ex/0411054.
- [4] J. Adams, et al., Phys. Rev. Lett. 97 (2006) 152302, arXiv:nucl-ex/0602011.
- [5] A. Adare, et al., Phys. Rev. Lett. 107 (2011) 172301, arXiv:1105.5112.
- [6] J. Jalilian-Marian, Y.V. Kovchegov, Prog. Part. Nucl. Phys. 56 (2006) 104, arXiv:hep-ph/0505052.
- [7] F. Gelis, E. Iancu, J. Jalilian-Marian, R. Venugopalan, Annu. Rev. Nucl. Part. Sci. 60 (2010) 463, arXiv:1002.0333.
- [8] D. Kharzeev, Y. Kovchegov, K. Tuchin, Phys. Lett. B 599 (2004) 23, arXiv:hep-ph/0405045.
- [9] K. Eskola, H. Paukkunen, C. Salgado, J. High Energy Phys. 0904 (2009) 065, arXiv:0902.4154.
- [10] B. Kopeliovich, et al., Phys. Rev. C 72 (2005) 054606, arXiv:hep-ph/0501260.
- [11] J.-W. Qiu, I. Vitev, Phys. Lett. B 632 (2006) 507, arXiv:hep-ph/0405068.
- [12] M. Cacciari, G.P. Salam, G. Soyez, J. High Energy Phys. 0804 (2008) 063, arXiv:0802.1189.
- [13] S.S. Adler, et al., Phys. Rev. Lett. 98 (2007) 172302, arXiv:nucl-ex/0610036.
- [14] B.B. Back, et al., Phys. Rev. C 72 (2005) 031901, arXiv:nucl-ex/0409021.
- [15] M.L. Miller, K. Reygers, S.J. Sanders, P. Steinberg, Annu. Rev. Nucl. Part. Sci. 57 (2007) 205, arXiv:nucl-ex/0701025.
- [16] ATLAS Collaboration, J. Instrum. 3 (2008) S08003, <http://dx.doi.org/10.1088/1748-0221/3/08/S08003>.
- [17] ATLAS Collaboration, Eur. Phys. J. C 70 (2010) 787, arXiv:1004.5293.
- [18] ATLAS Collaboration, Eur. Phys. J. C 72 (2012) 1849, arXiv:1110.1530.
- [19] ATLAS Collaboration, New J. Phys. 13 (2010) 053033, arXiv:1012.5104.
- [20] ATLAS Collaboration, Phys. Lett. B 710 (2012) 363, arXiv:1108.6027.
- [21] B. Alver, M. Baker, C. Loizides, P. Steinberg, The PHOBOS Glauber Monte Carlo, arXiv:0805.4411.
- [22] T. Sjostrand, S. Mrenna, P.Z. Skands, J. High Energy Phys. 0605 (2006) 026, arXiv:hep-ph/0603175.

- [23] T. Sjostrand, S. Mrenna, P.Z. Skands, *Comput. Phys. Commun.* 178 (2008) 852, arXiv:0710.3820.
- [24] A. Bialas, M. Bleszynski, W. Czyz, *Nucl. Phys. B* 111 (1976) 461, [http://dx.doi.org/10.1016/0550-3213\(76\)90329-1](http://dx.doi.org/10.1016/0550-3213(76)90329-1).
- [25] P. Steinberg, Inclusive pseudorapidity distributions in $p(d) + A$ collisions modeled with shifted rapidity distributions, arXiv:nucl-ex/0703002.
- [26] ATLAS Collaboration, ATL-PHYS-PUB-2012-003, <http://cds.cern.ch/record/1474107>.
- [27] J. Pumplin, et al., *J. High Energy Phys.* 0207 (2002) 012, arXiv:hep-ph/0201195.
- [28] GEANT4 Collaboration, S. Agostinelli, et al., *Nucl. Instrum. Methods A* 506 (2003) 250.
- [29] ATLAS Collaboration, *Eur. Phys. J. C* 70 (2010) 823, arXiv:1005.4568.
- [30] ATLAS Collaboration, *Phys. Lett. B* 719 (2013) 220, arXiv:1208.1967.
- [31] ATLAS Collaboration, *Phys. Rev. Lett.* 111 (2013) 152301, arXiv:1306.6469.
- [32] ATLAS Collaboration, *Eur. Phys. J. C* 73 (2013) 2304, arXiv:1112.6426.
- [33] ATLAS Collaboration, *Eur. Phys. J. C* 75 (2015) 1, arXiv:1406.0076.
- [34] ATLAS Collaboration, *Eur. Phys. J. C* 73 (2013) 2509, arXiv:1304.4739.
- [35] ATLAS Collaboration, *Phys. Rev. D* 86 (2012) 014022, arXiv:1112.6297.
- [36] ATLAS Collaboration, *Eur. Phys. J. C* 73 (2013) 2306, arXiv:1210.6210.
- [37] S. van der Meer, CERN-ISR-PO-68-31, <http://cds.cern.ch/record/296752>.
- [38] ATLAS Collaboration, *Eur. Phys. J. C* 73 (2013) 2518, arXiv:1302.4393.
- [39] H.-L. Lai, M. Guzzi, J. Huston, Z. Li, P.M. Nadolsky, et al., *Phys. Rev. D* 82 (2010) 074024, arXiv:1007.2241.
- [40] J. Albacete, N. Armesto, R. Baier, G. Barnafoldi, J. Barrette, et al., *Int. J. Mod. Phys. E* 22 (2013) 1330007, arXiv:1301.3395.
- [41] M. Alvioli, M. Strikman, *Phys. Lett. B* 722 (2013) 347, arXiv:1301.0728.
- [42] M. Alvioli, L. Frankfurt, V. Guzey, M. Strikman, *Phys. Rev. C* 90 (2014) 034914, arXiv:1402.2868.
- [43] C.E. Coleman-Smith, B. Müller, *Phys. Rev. D* 89 (2014) 025019, arXiv:1307.5911.
- [44] A. Bzdak, V. Skokov, S. Bathe, Centrality dependence of high energy jets in $p + Pb$ collisions at the LHC, arXiv:1408.3156.
- [45] M. Alvioli, B. Cole, L. Frankfurt, D. Perepelitsa, M. Strikman, Evidence for x -dependent proton color fluctuations in pA collisions at the LHC, arXiv:1409.7381.

ATLAS Collaboration

G. Aad⁸⁴, B. Abbott¹¹², J. Abdallah¹⁵², S. Abdel Khalek¹¹⁶, O. Abdinov¹¹, R. Aben¹⁰⁶, B. Abi¹¹³, M. Abolins⁸⁹, O.S. AbouZeid¹⁵⁹, H. Abramowicz¹⁵⁴, H. Abreu¹⁵³, R. Abreu³⁰, Y. Abulaiti^{147a,147b}, B.S. Acharya^{165a,165b,a}, L. Adamczyk^{38a}, D.L. Adams²⁵, J. Adelman¹⁷⁷, S. Adomeit⁹⁹, T. Adye¹³⁰, T. Agatonovic-Jovin^{13a}, J.A. Aguilar-Saavedra^{125a,125f}, M. Agustoni¹⁷, S.P. Ahlen²², F. Ahmadov^{64,b}, G. Aielli^{134a,134b}, H. Akerstedt^{147a,147b}, T.P.A. Åkesson⁸⁰, G. Akimoto¹⁵⁶, A.V. Akimov⁹⁵, G.L. Alberghi^{20a,20b}, J. Albert¹⁷⁰, S. Albrand⁵⁵, M.J. Alconada Verzini⁷⁰, M. Alekса³⁰, I.N. Aleksandrov⁶⁴, C. Alexa^{26a}, G. Alexander¹⁵⁴, G. Alexandre⁴⁹, T. Alexopoulos¹⁰, M. Alhroob^{165a,165c}, G. Alimonti^{90a}, L. Alio⁸⁴, J. Alison³¹, B.M.M. Allbrooke¹⁸, L.J. Allison⁷¹, P.P. Allport⁷³, J. Almond⁸³, A. Aloisio^{103a,103b}, A. Alonso³⁶, F. Alonso⁷⁰, C. Alpigiani⁷⁵, A. Altheimer³⁵, B. Alvarez Gonzalez⁸⁹, M.G. Alviggi^{103a,103b}, K. Amako⁶⁵, Y. Amaral Coutinho^{24a}, C. Amelung²³, D. Amidei⁸⁸, S.P. Amor Dos Santos^{125a,125c}, A. Amorim^{125a,125b}, S. Amoroso⁴⁸, N. Amram¹⁵⁴, G. Amundsen²³, C. Anastopoulos¹⁴⁰, L.S. Ancu⁴⁹, N. Andari³⁰, T. Andeen³⁵, C.F. Anders^{58b}, G. Anders³⁰, K.J. Anderson³¹, A. Andreazza^{90a,90b}, V. Andrei^{58a}, X.S. Anduaga⁷⁰, S. Angelidakis⁹, I. Angelozzi¹⁰⁶, P. Anger⁴⁴, A. Angerami³⁵, F. Anghinolfi³⁰, A.V. Anisenkov^{108,c}, N. Anjos^{125a}, A. Annovi⁴⁷, A. Antonaki⁹, M. Antonelli⁴⁷, A. Antonov⁹⁷, J. Antos^{145b}, F. Anulli^{133a}, M. Aoki⁶⁵, L. Aperio Bella¹⁸, R. Apolle^{119,d}, G. Arabidze⁸⁹, I. Aracena¹⁴⁴, Y. Arai⁶⁵, J.P. Araque^{125a}, A.T.H. Arce⁴⁵, J-F. Arguin⁹⁴, S. Argyropoulos⁴², M. Arik^{19a}, A.J. Armbruster³⁰, O. Arnaez³⁰, V. Arnal⁸¹, H. Arnold⁴⁸, M. Arratia²⁸, O. Arslan²¹, A. Artamonov⁹⁶, G. Artoni²³, S. Asai¹⁵⁶, N. Asbah⁴², A. Ashkenazi¹⁵⁴, B. Åsman^{147a,147b}, L. Asquith⁶, K. Assamagan²⁵, R. Astalos^{145a}, M. Atkinson¹⁶⁶, N.B. Atlay¹⁴², B. Auerbach⁶, K. Augsten¹²⁷, M. Aurousseau^{146b}, G. Avolio³⁰, G. Azuelos^{94,e}, Y. Azuma¹⁵⁶, M.A. Baak³⁰, A.E. Baas^{58a}, C. Bacci^{135a,135b}, H. Bachacou¹³⁷, K. Bachas¹⁵⁵, M. Backes³⁰, M. Backhaus³⁰, J. Backus Mayes¹⁴⁴, E. Badescu^{26a}, P. Bagiacchi^{133a,133b}, P. Bagnaia^{133a,133b}, Y. Bai^{33a}, T. Bain³⁵, J.T. Baines¹³⁰, O.K. Baker¹⁷⁷, P. Balek¹²⁸, F. Balli¹³⁷, E. Banas³⁹, Sw. Banerjee¹⁷⁴, A.A.E. Bannoura¹⁷⁶, V. Bansal¹⁷⁰, H.S. Bansil¹⁸, L. Barak¹⁷³, S.P. Baranov⁹⁵, E.L. Barberio⁸⁷, D. Barberis^{50a,50b}, M. Barbero⁸⁴, T. Barillari¹⁰⁰, M. Barisonzi¹⁷⁶, T. Barklow¹⁴⁴, N. Barlow²⁸, B.M. Barnett¹³⁰, R.M. Barnett¹⁵, Z. Barnovska⁵, A. Baroncelli^{135a}, G. Barone⁴⁹, A.J. Barr¹¹⁹, F. Barreiro⁸¹, J. Barreiro Guimarães da Costa⁵⁷, R. Bartoldus¹⁴⁴, A.E. Barton⁷¹, P. Bartos^{145a}, V. Bartsch¹⁵⁰, A. Bassalat¹¹⁶, A. Basye¹⁶⁶, R.L. Bates⁵³, J.R. Batley²⁸, M. Battaglia¹³⁸, M. Battistin³⁰, F. Bauer¹³⁷, H.S. Bawa^{144,f}, M.D. Beattie⁷¹, T. Beau⁷⁹, P.H. Beauchemin¹⁶², R. Beccherle^{123a,123b}, P. Bechtle²¹, H.P. Beck^{17,g}, K. Becker¹⁷⁶, S. Becker⁹⁹, M. Beckingham¹⁷¹, C. Becot¹¹⁶, A.J. Beddall^{19c}, A. Beddall^{19c}, S. Bedikian¹⁷⁷, V.A. Bednyakov⁶⁴, C.P. Bee¹⁴⁹, L.J. Beemster¹⁰⁶, T.A. Beermann¹⁷⁶, M. Begel²⁵, K. Behr¹¹⁹, C. Belanger-Champagne⁸⁶, P.J. Bell⁴⁹, W.H. Bell⁴⁹, G. Bella¹⁵⁴, L. Bellagamba^{20a}, A. Bellerive²⁹, M. Bellomo⁸⁵, K. Belotskiy⁹⁷, O. Beltramello³⁰, O. Benary¹⁵⁴, D. Benchekroun^{136a}, K. Bendtz^{147a,147b}, N. Benekos¹⁶⁶, Y. Benhammou¹⁵⁴, E. Benhar Noccioli⁴⁹, J.A. Benitez Garcia^{160b}, D.P. Benjamin⁴⁵, J.R. Bensinger²³, K. Benslama¹³¹, S. Bentvelsen¹⁰⁶, D. Berge¹⁰⁶, E. Bergeaas Kuutmann¹⁶⁷, N. Berger⁵, F. Berghaus¹⁷⁰, J. Beringer¹⁵, C. Bernard²², P. Bernat⁷⁷, C. Bernius⁷⁸, F.U. Bernlochner¹⁷⁰, T. Berry⁷⁶, P. Berta¹²⁸, C. Bertella⁸⁴, G. Bertoli^{147a,147b}, F. Bertolucci^{123a,123b}, C. Bertsche¹¹², D. Bertsche¹¹², M.I. Besana^{90a}, G.J. Besjes¹⁰⁵, O. Bessidskaia Bylund^{147a,147b}, M. Bessner⁴², N. Besson¹³⁷, C. Betancourt⁴⁸, S. Bethke¹⁰⁰, W. Bhimji⁴⁶,

- R.M. Bianchi ¹²⁴, L. Bianchini ²³, M. Bianco ³⁰, O. Biebel ⁹⁹, S.P. Bieniek ⁷⁷, K. Bierwagen ⁵⁴, J. Biesiada ¹⁵, M. Biglietti ^{135a}, J. Bilbao De Mendizabal ⁴⁹, H. Bilokon ⁴⁷, M. Bindi ⁵⁴, S. Binet ¹¹⁶, A. Bingul ^{19c}, C. Bini ^{133a,133b}, C.W. Black ¹⁵¹, J.E. Black ¹⁴⁴, K.M. Black ²², D. Blackburn ¹³⁹, R.E. Blair ⁶, J.-B. Blanchard ¹³⁷, T. Blazek ^{145a}, I. Bloch ⁴², C. Blocker ²³, W. Blum ^{82,*}, U. Blumenschein ⁵⁴, G.J. Bobbink ¹⁰⁶, V.S. Bobrovnikov ^{108,c}, S.S. Bocchetta ⁸⁰, A. Bocci ⁴⁵, C. Bock ⁹⁹, C.R. Boddy ¹¹⁹, M. Boehler ⁴⁸, T.T. Boek ¹⁷⁶, J.A. Bogaerts ³⁰, A.G. Bogdanchikov ¹⁰⁸, A. Bogouch ^{91,*}, C. Bohm ^{147a}, J. Bohm ¹²⁶, V. Boisvert ⁷⁶, T. Bold ^{38a}, V. Boldea ^{26a}, A.S. Boldyrev ⁹⁸, M. Bomben ⁷⁹, M. Bona ⁷⁵, M. Boonekamp ¹³⁷, A. Borisov ¹²⁹, G. Borissov ⁷¹, M. Borri ⁸³, S. Borroni ⁴², J. Bortfeldt ⁹⁹, V. Bortolotto ^{135a,135b}, K. Bos ¹⁰⁶, D. Boscherini ^{20a}, M. Bosman ¹², H. Boterenbrood ¹⁰⁶, J. Boudreau ¹²⁴, J. Bouffard ², E.V. Bouhova-Thacker ⁷¹, D. Boumediene ³⁴, C. Bourdarios ¹¹⁶, N. Bousson ¹¹³, S. Boutouil ^{136d}, A. Boveia ³¹, J. Boyd ³⁰, I.R. Boyko ⁶⁴, J. Bracinik ¹⁸, A. Brandt ⁸, G. Brandt ¹⁵, O. Brandt ^{58a}, U. Bratzler ¹⁵⁷, B. Brau ⁸⁵, J.E. Brau ¹¹⁵, H.M. Braun ^{176,*}, S.F. Brazzale ^{165a,165c}, B. Brelier ¹⁵⁹, K. Brendlinger ¹²¹, A.J. Brennan ⁸⁷, R. Brenner ¹⁶⁷, S. Bressler ¹⁷³, K. Bristow ^{146c}, T.M. Bristow ⁴⁶, D. Britton ⁵³, F.M. Brochu ²⁸, I. Brock ²¹, R. Brock ⁸⁹, C. Bromberg ⁸⁹, J. Bronner ¹⁰⁰, G. Brooijmans ³⁵, T. Brooks ⁷⁶, W.K. Brooks ^{32b}, J. Brosamer ¹⁵, E. Brost ¹¹⁵, J. Brown ⁵⁵, P.A. Bruckman de Renstrom ³⁹, D. Bruncko ^{145b}, R. Bruneliere ⁴⁸, S. Brunet ⁶⁰, A. Bruni ^{20a}, G. Bruni ^{20a}, M. Bruschi ^{20a}, L. Bryngemark ⁸⁰, T. Buanes ¹⁴, Q. Buat ¹⁴³, F. Bucci ⁴⁹, P. Buchholz ¹⁴², R.M. Buckingham ¹¹⁹, A.G. Buckley ⁵³, S.I. Buda ^{26a}, I.A. Budagov ⁶⁴, F. Buehrer ⁴⁸, L. Bugge ¹¹⁸, M.K. Bugge ¹¹⁸, O. Bulekov ⁹⁷, A.C. Bundred ⁷³, H. Burckhart ³⁰, S. Burdin ⁷³, B. Burghgrave ¹⁰⁷, S. Burke ¹³⁰, I. Burmeister ⁴³, E. Busato ³⁴, D. Büscher ⁴⁸, V. Büscher ⁸², P. Bussey ⁵³, C.P. Buszello ¹⁶⁷, B. Butler ⁵⁷, J.M. Butler ²², A.I. Butt ³, C.M. Buttar ⁵³, J.M. Butterworth ⁷⁷, P. Butti ¹⁰⁶, W. Buttlinger ²⁸, A. Buzatu ⁵³, M. Byszewski ¹⁰, S. Cabrera Urbán ¹⁶⁸, D. Caforio ^{20a,20b}, O. Cakir ^{4a}, P. Calafiura ¹⁵, A. Calandri ¹³⁷, G. Calderini ⁷⁹, P. Calfayan ⁹⁹, R. Calkins ¹⁰⁷, L.P. Caloba ^{24a}, D. Calvet ³⁴, S. Calvet ³⁴, R. Camacho Toro ⁴⁹, S. Camarda ⁴², D. Cameron ¹¹⁸, L.M. Caminada ¹⁵, R. Caminal Armadans ¹², S. Campana ³⁰, M. Campanelli ⁷⁷, A. Campoverde ¹⁴⁹, V. Canale ^{103a,103b}, A. Canepa ^{160a}, M. Cano Bret ⁷⁵, J. Cantero ⁸¹, R. Cantrill ^{125a}, T. Cao ⁴⁰, M.D.M. Capeans Garrido ³⁰, I. Caprini ^{26a}, M. Caprini ^{26a}, M. Capua ^{37a,37b}, R. Caputo ⁸², R. Cardarelli ^{134a}, T. Carli ³⁰, G. Carlino ^{103a}, L. Carminati ^{90a,90b}, S. Caron ¹⁰⁵, E. Carquin ^{32a}, G.D. Carrillo-Montoya ^{146c}, J.R. Carter ²⁸, J. Carvalho ^{125a,125c}, D. Casadei ⁷⁷, M.P. Casado ¹², M. Casolino ¹², E. Castaneda-Miranda ^{146b}, A. Castelli ¹⁰⁶, V. Castillo Gimenez ¹⁶⁸, N.F. Castro ^{125a}, P. Catastini ⁵⁷, A. Catinaccio ³⁰, J.R. Catmore ¹¹⁸, A. Cattai ³⁰, G. Cattani ^{134a,134b}, J. Caudron ⁸², S. Caugron ⁸⁹, V. Cavaliere ¹⁶⁶, D. Cavalli ^{90a}, M. Cavalli-Sforza ¹², V. Cavasinni ^{123a,123b}, F. Ceradini ^{135a,135b}, B.C. Cerio ⁴⁵, K. Cerny ¹²⁸, A.S. Cerqueira ^{24b}, A. Cerri ¹⁵⁰, L. Cerrito ⁷⁵, F. Cerutti ¹⁵, M. Cerv ³⁰, A. Cervelli ¹⁷, S.A. Cetin ^{19b}, A. Chafaq ^{136a}, D. Chakraborty ¹⁰⁷, I. Chalupkova ¹²⁸, P. Chang ¹⁶⁶, B. Chapleau ⁸⁶, J.D. Chapman ²⁸, D. Charfeddine ¹¹⁶, D.G. Charlton ¹⁸, C.C. Chau ¹⁵⁹, C.A. Chavez Barajas ¹⁵⁰, S. Cheatham ⁸⁶, A. Chegwidden ⁸⁹, S. Chekanov ⁶, S.V. Chekulaev ^{160a}, G.A. Chelkov ^{64,h}, M.A. Chelstowska ⁸⁸, C. Chen ⁶³, H. Chen ²⁵, K. Chen ¹⁴⁹, L. Chen ^{33d,i}, S. Chen ^{33c}, X. Chen ^{146c}, Y. Chen ⁶⁶, Y. Chen ³⁵, H.C. Cheng ⁸⁸, Y. Cheng ³¹, A. Cheplakov ⁶⁴, R. Cherkaoui El Moursli ^{136e}, V. Chernyatin ^{25,*}, E. Cheu ⁷, L. Chevalier ¹³⁷, V. Chiarella ⁴⁷, G. Chiefari ^{103a,103b}, J.T. Childers ⁶, A. Chilingarov ⁷¹, G. Chiodini ^{72a}, A.S. Chisholm ¹⁸, R.T. Chislett ⁷⁷, A. Chitan ^{26a}, M.V. Chizhov ⁶⁴, S. Chouridou ⁹, B.K.B. Chow ⁹⁹, D. Chromek-Burckhart ³⁰, M.L. Chu ¹⁵², J. Chudoba ¹²⁶, J.J. Chwastowski ³⁹, L. Chytka ¹¹⁴, G. Ciapetti ^{133a,133b}, A.K. Ciftci ^{4a}, R. Ciftci ^{4a}, D. Cinca ⁵³, V. Cindro ⁷⁴, A. Ciocio ¹⁵, P. Cirkovic ^{13b}, Z.H. Citron ¹⁷³, M. Citterio ^{90a}, M. Ciubancan ^{26a}, A. Clark ⁴⁹, P.J. Clark ⁴⁶, R.N. Clarke ¹⁵, W. Cleland ¹²⁴, J.C. Clemens ⁸⁴, C. Clement ^{147a,147b}, Y. Coadou ⁸⁴, M. Cobal ^{165a,165c}, A. Coccaro ¹³⁹, J. Cochran ⁶³, L. Coffey ²³, J.G. Cogan ¹⁴⁴, J. Coggshall ¹⁶⁶, B. Cole ³⁵, S. Cole ¹⁰⁷, A.P. Colijn ¹⁰⁶, J. Collot ⁵⁵, T. Colombo ^{58c}, G. Colon ⁸⁵, G. Compostella ¹⁰⁰, P. Conde Muiño ^{125a,125b}, E. Coniavitis ⁴⁸, M.C. Conidi ¹², S.H. Connell ^{146b}, I.A. Connolly ⁷⁶, S.M. Consonni ^{90a,90b}, V. Consorti ⁴⁸, S. Constantinescu ^{26a}, C. Conta ^{120a,120b}, G. Conti ⁵⁷, F. Conventi ^{103a,j}, M. Cooke ¹⁵, B.D. Cooper ⁷⁷, A.M. Cooper-Sarkar ¹¹⁹, N.J. Cooper-Smith ⁷⁶, K. Copic ¹⁵, T. Cornelissen ¹⁷⁶, M. Corradi ^{20a}, F. Corriveau ^{86,k}, A. Corso-Radu ¹⁶⁴, A. Cortes-Gonzalez ¹², G. Cortiana ¹⁰⁰, G. Costa ^{90a}, M.J. Costa ¹⁶⁸, D. Costanzo ¹⁴⁰, D. Côté ⁸, G. Cottin ²⁸, G. Cowan ⁷⁶, B.E. Cox ⁸³, K. Cranmer ¹⁰⁹, G. Cree ²⁹, S. Crépé-Renaudin ⁵⁵, F. Crescioli ⁷⁹, W.A. Cribbs ^{147a,147b}, M. Crispin Ortuzar ¹¹⁹, M. Cristinziani ²¹, V. Croft ¹⁰⁵, G. Crosetti ^{37a,37b}, C.-M. Cuciuc ^{26a}, T. Cuhadar Donszelmann ¹⁴⁰, J. Cummings ¹⁷⁷, M. Curatolo ⁴⁷, C. Cuthbert ¹⁵¹, H. Czirr ¹⁴², P. Czodrowski ³, Z. Czyczula ¹⁷⁷, S. D'Auria ⁵³, M. D'Onofrio ⁷³,

- M.J. Da Cunha Sargedas De Sousa 125a,125b, C. Da Via 83, W. Dabrowski 38a, A. Dafinca 119, T. Dai 88, O. Dale 14, F. Dallaire 94, C. Dallapiccola 85, M. Dam 36, A.C. Daniells 18, M. Dano Hoffmann 137, V. Dao 48, G. Darbo 50a, S. Darmora 8, J. Dassoulas 42, A. Dattagupta 60, W. Davey 21, C. David 170, T. Davidek 128, E. Davies 119,d, M. Davies 154, O. Davignon 79, A.R. Davison 77, P. Davison 77, Y. Davygora 58a, E. Dawe 143, I. Dawson 140, R.K. Daya-Ishmukhametova 85, K. De 8, R. de Asmundis 103a, S. De Castro 20a,20b, S. De Cecco 79, N. De Groot 105, P. de Jong 106, H. De la Torre 81, F. De Lorenzi 63, L. De Nooij 106, D. De Pedis 133a, A. De Salvo 133a, U. De Sanctis 165a,165b, A. De Santo 150, J.B. De Vivie De Regie 116, W.J. Dearnaley 71, R. Debbe 25, C. Debenedetti 138, B. Dechenaux 55, D.V. Dedovich 64, I. Deigaard 106, J. Del Peso 81, T. Del Prete 123a,123b, F. Deliot 137, C.M. Delitzsch 49, M. Deliyergiyev 74, A. Dell'Acqua 30, L. Dell'Asta 22, M. Dell'Orso 123a,123b, M. Della Pietra 103a,j, D. della Volpe 49, M. Delmastro 5, P.A. Delsart 55, C. Deluca 106, S. Demers 177, M. Demichev 64, A. Demilly 79, S.P. Denisov 129, D. Derendarz 39, J.E. Derkaoui 136d, F. Derue 79, P. Dervan 73, K. Desch 21, C. Deterre 42, P.O. Deviveiros 106, A. Dewhurst 130, S. Dhaliwal 106, A. Di Ciaccio 134a,134b, L. Di Ciaccio 5, A. Di Domenico 133a,133b, C. Di Donato 103a,103b, A. Di Girolamo 30, B. Di Girolamo 30, A. Di Mattia 153, B. Di Micco 135a,135b, R. Di Nardo 47, A. Di Simone 48, R. Di Sipio 20a,20b, D. Di Valentino 29, F.A. Dias 46, M.A. Diaz 32a, E.B. Diehl 88, J. Dietrich 42, T.A. Dietzsch 58a, S. Diglio 84, A. Dimitrijevska 13a, J. Dingfelder 21, C. Dionisi 133a,133b, P. Dita 26a, S. Dita 26a, F. Dittus 30, F. Djama 84, T. Djobava 51b, J.I. Djuvsland 58a, M.A.B. do Vale 24c, A. Do Valle Wemans 125a,125g, T.K.O. Doan 5, D. Dobos 30, C. Doglioni 49, T. Doherty 53, T. Dohmae 156, J. Dolejsi 128, Z. Dolezal 128, B.A. Dolgoshein 97,* M. Donadelli 24d, S. Donati 123a,123b, P. Dondero 120a,120b, J. Donini 34, J. Dopke 130, A. Doria 103a, M.T. Dova 70, A.T. Doyle 53, M. Dris 10, J. Dubbert 88, S. Dube 15, E. Dubreuil 34, E. Duchovni 173, G. Duckeck 99, O.A. Ducu 26a, D. Duda 176, A. Dudarev 30, F. Dudziak 63, L. Duflot 116, L. Duguid 76, M. Dührssen 30, M. Dunford 58a, H. Duran Yildiz 4a, M. Düren 52, A. Durglishvili 51b, M. Dwuznik 38a, M. Dyndal 38a, J. Ebke 99, W. Edson 2, N.C. Edwards 46, W. Ehrenfeld 21, T. Eifert 144, G. Eigen 14, K. Einsweiler 15, T. Ekelof 167, M. El Kacimi 136c, M. Ellert 167, S. Elles 5, F. Ellinghaus 82, N. Ellis 30, J. Elmsheuser 99, M. Elsing 30, D. Emeliyanov 130, Y. Enari 156, O.C. Endner 82, M. Endo 117, R. Engelmann 149, J. Erdmann 177, A. Ereditato 17, D. Eriksson 147a, G. Ernis 176, J. Ernst 2, M. Ernst 25, J. Ernwein 137, D. Errede 166, S. Errede 166, E. Ertel 82, M. Escalier 116, H. Esch 43, C. Escobar 124, B. Esposito 47, A.I. Etienne 137, E. Etzion 154, H. Evans 60, A. Ezhilov 122, L. Fabbri 20a,20b, G. Facini 31, R.M. Fakhrutdinov 129, S. Falciano 133a, R.J. Falla 77, J. Faltova 128, Y. Fang 33a, M. Fanti 90a,90b, A. Farbin 8, A. Farilla 135a, T. Farooque 12, S. Farrell 15, S.M. Farrington 171, P. Farthouat 30, F. Fassi 136e, P. Fassnacht 30, D. Fassouliotis 9, A. Favareto 50a,50b, L. Fayard 116, P. Federic 145a, O.L. Fedin 122,l, W. Fedorko 169, M. Fehling-Kaschek 48, S. Feigl 30, L. Feligioni 84, C. Feng 33d, E.J. Feng 6, H. Feng 88, A.B. Fenyuk 129, S. Fernandez Perez 30, S. Ferrag 53, J. Ferrando 53, A. Ferrari 167, P. Ferrari 106, R. Ferrari 120a, D.E. Ferreira de Lima 53, A. Ferrer 168, D. Ferrere 49, C. Ferretti 88, A. Ferretto Parodi 50a,50b, M. Fiascaris 31, F. Fiedler 82, A. Filipčič 74, M. Filipuzzi 42, F. Filthaut 105, M. Fincke-Keeler 170, K.D. Finelli 151, M.C.N. Fiolhais 125a,125c, L. Fiorini 168, A. Firan 40, A. Fischer 2, J. Fischer 176, W.C. Fisher 89, E.A. Fitzgerald 23, M. Flechl 48, I. Fleck 142, P. Fleischmann 88, S. Fleischmann 176, G.T. Fletcher 140, G. Fletcher 75, T. Flick 176, A. Floderus 80, L.R. Flores Castillo 174,m, A.C. Florez Bustos 160b, M.J. Flowerdew 100, A. Formica 137, A. Forti 83, D. Fortin 160a, D. Fournier 116, H. Fox 71, S. Fracchia 12, P. Francavilla 79, M. Franchini 20a,20b, S. Franchino 30, D. Francis 30, L. Franconi 118, M. Franklin 57, S. Franz 61, M. Fraternali 120a,120b, S.T. French 28, C. Friedrich 42, F. Friedrich 44, D. Froidevaux 30, J.A. Frost 28, C. Fukunaga 157, E. Fullana Torregrosa 82, B.G. Fulsom 144, J. Fuster 168, C. Gabaldon 55, O. Gabizon 173, A. Gabrielli 20a,20b, A. Gabrielli 133a,133b, S. Gadatsch 106, S. Gadomski 49, G. Gagliardi 50a,50b, P. Gagnon 60, C. Galea 105, B. Galhardo 125a,125c, E.J. Gallas 119, V. Gallo 17, B.J. Gallop 130, P. Gallus 127, G. Galster 36, K.K. Gan 110, R.P. Gandajula 62, J. Gao 33b, Y.S. Gao 144,f, F.M. Garay Walls 46, F. Garberson 177, C. García 168, J.E. García Navarro 168, M. Garcia-Sciveres 15, R.W. Gardner 31, N. Garelli 144, V. Garonne 30, C. Gatti 47, G. Gaudio 120a, B. Gaur 142, L. Gauthier 94, P. Gauzzi 133a,133b, I.L. Gavrilenko 95, C. Gay 169, G. Gaycken 21, E.N. Gazis 10, P. Ge 33d, Z. Gecse 169, C.N.P. Gee 130, D.A.A. Geerts 106, Ch. Geich-Gimbel 21, K. Gellerstedt 147a,147b, C. Gemme 50a, A. Gemmell 53, M.H. Genest 55, S. Gentile 133a,133b, M. George 54, S. George 76, D. Gerbaudo 164, A. Gershon 154, H. Ghazlane 136b, N. Ghodbane 34, B. Giacobbe 20a, S. Giagu 133a,133b, V. Giangiobbe 12, P. Giannetti 123a,123b, F. Gianotti 30, B. Gibbard 25, S.M. Gibson 76, M. Gilchriese 15, T.P.S. Gillam 28,

- D. Gillberg ³⁰, G. Gilles ³⁴, D.M. Gingrich ^{3,e}, N. Giokaris ⁹, M.P. Giordani ^{165a,165c}, R. Giordano ^{103a,103b}, F.M. Giorgi ^{20a}, F.M. Giorgi ¹⁶, P.F. Giraud ¹³⁷, D. Giugni ^{90a}, C. Giuliani ⁴⁸, M. Giulini ^{58b}, B.K. Gjelsten ¹¹⁸, S. Gkaitatzis ¹⁵⁵, I. Gkialas ¹⁵⁵, L.K. Gladilin ⁹⁸, C. Glasman ⁸¹, J. Glatzer ³⁰, P.C.F. Glaysher ⁴⁶, A. Glazov ⁴², G.L. Glonti ⁶⁴, M. Goblirsch-Kolb ¹⁰⁰, J.R. Goddard ⁷⁵, J. Godfrey ¹⁴³, J. Godlewski ³⁰, C. Goeringer ⁸², S. Goldfarb ⁸⁸, T. Golling ¹⁷⁷, D. Golubkov ¹²⁹, A. Gomes ^{125a,125b,125d}, L.S. Gomez Fajardo ⁴², R. Gonçalo ^{125a}, J. Goncalves Pinto Firmino Da Costa ¹³⁷, L. Gonella ²¹, S. González de la Hoz ¹⁶⁸, G. Gonzalez Parra ¹², S. Gonzalez-Sevilla ⁴⁹, L. Goossens ³⁰, P.A. Gorbounov ⁹⁶, H.A. Gordon ²⁵, I. Gorelov ¹⁰⁴, B. Gorini ³⁰, E. Gorini ^{72a,72b}, A. Gorišek ⁷⁴, E. Gornicki ³⁹, A.T. Goshaw ⁶, C. Gössling ⁴³, M.I. Gostkin ⁶⁴, M. Gouighri ^{136a}, D. Goujdami ^{136c}, M.P. Goulette ⁴⁹, A.G. Goussiou ¹³⁹, C. Goy ⁵, S. Gozpinar ²³, H.M.X. Grabas ¹³⁷, L. Gruber ⁵⁴, I. Grabowska-Bold ^{38a}, P. Grafström ^{20a,20b}, K.-J. Grahn ⁴², J. Gramling ⁴⁹, E. Gramstad ¹¹⁸, S. Grancagnolo ¹⁶, V. Grassi ¹⁴⁹, V. Gratchev ¹²², H.M. Gray ³⁰, E. Graziani ^{135a}, O.G. Grebenyuk ¹²², Z.D. Greenwood ^{78,n}, K. Gregersen ⁷⁷, I.M. Gregor ⁴², P. Grenier ¹⁴⁴, J. Griffiths ⁸, A.A. Grillo ¹³⁸, K. Grimm ⁷¹, S. Grinstein ^{12,o}, Ph. Gris ³⁴, Y.V. Grishkevich ⁹⁸, J.-F. Grivaz ¹¹⁶, J.P. Grohs ⁴⁴, A. Grohsjean ⁴², E. Gross ¹⁷³, J. Grosse-Knetter ⁵⁴, G.C. Grossi ^{134a,134b}, J. Groth-Jensen ¹⁷³, Z.J. Grout ¹⁵⁰, L. Guan ^{33b}, J. Guenther ¹²⁷, F. Guescini ⁴⁹, D. Guest ¹⁷⁷, O. Gueta ¹⁵⁴, C. Guicheney ³⁴, E. Guido ^{50a,50b}, T. Guillemin ¹¹⁶, S. Guindon ², U. Gul ⁵³, C. Gumpert ⁴⁴, J. Guo ³⁵, S. Gupta ¹¹⁹, P. Gutierrez ¹¹², N.G. Gutierrez Ortiz ⁵³, C. Gutschow ⁷⁷, N. Guttman ¹⁵⁴, C. Guyot ¹³⁷, C. Gwenlan ¹¹⁹, C.B. Gwilliam ⁷³, A. Haas ¹⁰⁹, C. Haber ¹⁵, H.K. Hadavand ⁸, N. Haddad ^{136e}, P. Haefner ²¹, S. Hageböck ²¹, Z. Hajduk ³⁹, H. Hakobyan ¹⁷⁸, M. Haleem ⁴², D. Hall ¹¹⁹, G. Halladjian ⁸⁹, K. Hamacher ¹⁷⁶, P. Hamal ¹¹⁴, K. Hamano ¹⁷⁰, M. Hamer ⁵⁴, A. Hamilton ^{146a}, S. Hamilton ¹⁶², G.N. Hamity ^{146c}, P.G. Hamnett ⁴², L. Han ^{33b}, K. Hanagaki ¹¹⁷, K. Hanawa ¹⁵⁶, M. Hance ¹⁵, P. Hanke ^{58a}, R. Hanna ¹³⁷, J.B. Hansen ³⁶, J.D. Hansen ³⁶, P.H. Hansen ³⁶, K. Hara ¹⁶¹, A.S. Hard ¹⁷⁴, T. Harenberg ¹⁷⁶, F. Hariri ¹¹⁶, S. Harkusha ⁹¹, D. Harper ⁸⁸, R.D. Harrington ⁴⁶, O.M. Harris ¹³⁹, P.F. Harrison ¹⁷¹, F. Hartjes ¹⁰⁶, M. Hasegawa ⁶⁶, S. Hasegawa ¹⁰², Y. Hasegawa ¹⁴¹, A. Hasib ¹¹², S. Hassani ¹³⁷, S. Haug ¹⁷, M. Hauschild ³⁰, R. Hauser ⁸⁹, M. Havranek ¹²⁶, C.M. Hawkes ¹⁸, R.J. Hawkings ³⁰, A.D. Hawkins ⁸⁰, T. Hayashi ¹⁶¹, D. Hayden ⁸⁹, C.P. Hays ¹¹⁹, H.S. Hayward ⁷³, S.J. Haywood ¹³⁰, S.J. Head ¹⁸, T. Heck ⁸², V. Hedberg ⁸⁰, L. Heelan ⁸, S. Heim ¹²¹, T. Heim ¹⁷⁶, B. Heinemann ¹⁵, L. Heinrich ¹⁰⁹, J. Hejbal ¹²⁶, L. Helary ²², C. Heller ⁹⁹, M. Heller ³⁰, S. Hellman ^{147a,147b}, D. Hellmich ²¹, C. Helsens ³⁰, J. Henderson ¹¹⁹, R.C.W. Henderson ⁷¹, Y. Heng ¹⁷⁴, C. Hengler ⁴², A. Henrichs ¹⁷⁷, A.M. Henriques Correia ³⁰, S. Henrot-Versille ¹¹⁶, C. Hensel ⁵⁴, G.H. Herbert ¹⁶, Y. Hernández Jiménez ¹⁶⁸, R. Herrberg-Schubert ¹⁶, G. Herten ⁴⁸, R. Hertenberger ⁹⁹, L. Hervas ³⁰, G.G. Hesketh ⁷⁷, N.P. Hessey ¹⁰⁶, R. Hickling ⁷⁵, E. Higón-Rodríguez ¹⁶⁸, E. Hill ¹⁷⁰, J.C. Hill ²⁸, K.H. Hiller ⁴², S. Hillert ²¹, S.J. Hillier ¹⁸, I. Hinchliffe ¹⁵, E. Hines ¹²¹, M. Hirose ¹⁵⁸, D. Hirschbuehl ¹⁷⁶, J. Hobbs ¹⁴⁹, N. Hod ¹⁰⁶, M.C. Hodgkinson ¹⁴⁰, P. Hodgson ¹⁴⁰, A. Hoecker ³⁰, M.R. Hoeferkamp ¹⁰⁴, F. Hoenig ⁹⁹, J. Hoffman ⁴⁰, D. Hoffmann ⁸⁴, M. Hohlfeld ⁸², T.R. Holmes ¹⁵, T.M. Hong ¹²¹, L. Hooft van Huysduynen ¹⁰⁹, J.-Y. Hostachy ⁵⁵, S. Hou ¹⁵², A. Hoummada ^{136a}, J. Howard ¹¹⁹, J. Howarth ⁴², M. Hrabovsky ¹¹⁴, I. Hristova ¹⁶, J. Hrivnac ¹¹⁶, T. Hrynn'ova ⁵, C. Hsu ^{146c}, P.J. Hsu ⁸², S.-C. Hsu ¹³⁹, D. Hu ³⁵, X. Hu ⁸⁸, Y. Huang ⁴², Z. Hubacek ³⁰, F. Hubaut ⁸⁴, F. Huegging ²¹, T.B. Huffman ¹¹⁹, E.W. Hughes ³⁵, G. Hughes ⁷¹, M. Huhtinen ³⁰, T.A. Hülsing ⁸², M. Hurwitz ¹⁵, N. Huseynov ^{64,b}, J. Huston ⁸⁹, J. Huth ⁵⁷, G. Iacobucci ⁴⁹, G. Iakovidis ¹⁰, I. Ibragimov ¹⁴², L. Iconomidou-Fayard ¹¹⁶, E. Ideal ¹⁷⁷, P. Iengo ^{103a}, O. Igonkina ¹⁰⁶, T. Iizawa ¹⁷², Y. Ikegami ⁶⁵, K. Ikematsu ¹⁴², M. Ikeno ⁶⁵, Y. Ilchenko ^{31,p}, D. Iliadis ¹⁵⁵, N. Ilic ¹⁵⁹, Y. Inamaru ⁶⁶, T. Ince ¹⁰⁰, P. Ioannou ⁹, M. Iodice ^{135a}, K. Iordanidou ⁹, V. Ippolito ⁵⁷, A. Irles Quiles ¹⁶⁸, C. Isaksson ¹⁶⁷, M. Ishino ⁶⁷, M. Ishitsuka ¹⁵⁸, R. Ishmukhametov ¹¹⁰, C. Issever ¹¹⁹, S. Istiñ ^{19a}, J.M. Iturbe Ponce ⁸³, R. Iuppa ^{134a,134b}, J. Ivarsson ⁸⁰, W. Iwanski ³⁹, H. Iwasaki ⁶⁵, J.M. Izen ⁴¹, V. Izzo ^{103a}, B. Jackson ¹²¹, M. Jackson ⁷³, P. Jackson ¹, M.R. Jaekel ³⁰, V. Jain ², K. Jakobs ⁴⁸, S. Jakobsen ³⁰, T. Jakoubek ¹²⁶, J. Jakubek ¹²⁷, D.O. Jamin ¹⁵², D.K. Jana ⁷⁸, E. Jansen ⁷⁷, H. Jansen ³⁰, J. Janssen ²¹, M. Janus ¹⁷¹, G. Jarlskog ⁸⁰, N. Javadov ^{64,b}, T. Javůrek ⁴⁸, L. Jeanty ¹⁵, J. Jejelava ^{51a,q}, G.-Y. Jeng ¹⁵¹, D. Jennens ⁸⁷, P. Jenni ^{48,r}, J. Jentzsch ⁴³, C. Jeske ¹⁷¹, S. Jézéquel ⁵, H. Ji ¹⁷⁴, J. Jia ¹⁴⁹, Y. Jiang ^{33b}, M. Jimenez Belenguer ⁴², S. Jin ^{33a}, A. Jinaru ^{26a}, O. Jinnouchi ¹⁵⁸, M.D. Joergensen ³⁶, K.E. Johansson ^{147a,147b}, P. Johansson ¹⁴⁰, K.A. Johns ⁷, K. Jon-And ^{147a,147b}, G. Jones ¹⁷¹, R.W.L. Jones ⁷¹, T.J. Jones ⁷³, J. Jongmanns ^{58a}, P.M. Jorge ^{125a,125b}, K.D. Joshi ⁸³, J. Jovicevic ¹⁴⁸, X. Ju ¹⁷⁴, C.A. Jung ⁴³, R.M. Jungst ³⁰, P. Jussel ⁶¹, A. Juste Rozas ^{12,o}, M. Kaci ¹⁶⁸, A. Kaczmarśka ³⁹, M. Kado ¹¹⁶, H. Kagan ¹¹⁰, M. Kagan ¹⁴⁴, E. Kajomovitz ⁴⁵, C.W. Kalderon ¹¹⁹, S. Kama ⁴⁰, A. Kamenshchikov ¹²⁹, N. Kanaya ¹⁵⁶,

- M. Kaneda ³⁰, S. Kaneti ²⁸, V.A. Kantserov ⁹⁷, J. Kanzaki ⁶⁵, B. Kaplan ¹⁰⁹, A. Kapliy ³¹, D. Kar ⁵³,
 K. Karakostas ¹⁰, N. Karastathis ¹⁰, M. Karnevskiy ⁸², S.N. Karpov ⁶⁴, Z.M. Karpova ⁶⁴, K. Karthik ¹⁰⁹,
 V. Kartvelishvili ⁷¹, A.N. Karyukhin ¹²⁹, L. Kashif ¹⁷⁴, G. Kasieczka ^{58b}, R.D. Kass ¹¹⁰, A. Kastanas ¹⁴,
 Y. Kataoka ¹⁵⁶, A. Katre ⁴⁹, J. Katzy ⁴², V. Kaushik ⁷, K. Kawagoe ⁶⁹, T. Kawamoto ¹⁵⁶, G. Kawamura ⁵⁴,
 S. Kazama ¹⁵⁶, V.F. Kazanin ¹⁰⁸, M.Y. Kazarinov ⁶⁴, R. Keeler ¹⁷⁰, R. Kehoe ⁴⁰, M. Keil ⁵⁴, J.S. Keller ⁴²,
 J.J. Kempster ⁷⁶, H. Keoshkerian ⁵, O. Kepka ¹²⁶, B.P. Kerševan ⁷⁴, S. Kersten ¹⁷⁶, K. Kessoku ¹⁵⁶,
 J. Keung ¹⁵⁹, F. Khalil-zada ¹¹, H. Khandanyan ^{147a,147b}, A. Khanov ¹¹³, A. Khodinov ⁹⁷, A. Khomich ^{58a},
 T.J. Khoo ²⁸, G. Khoriauli ²¹, A. Khoroshilov ¹⁷⁶, V. Khovanskii ⁹⁶, E. Khramov ⁶⁴, J. Khubua ^{51b}, H.Y. Kim ⁸,
 H. Kim ^{147a,147b}, S.H. Kim ¹⁶¹, N. Kimura ¹⁷², O. Kind ¹⁶, B.T. King ⁷³, M. King ¹⁶⁸, R.S.B. King ¹¹⁹,
 S.B. King ¹⁶⁹, J. Kirk ¹³⁰, A.E. Kiryunin ¹⁰⁰, T. Kishimoto ⁶⁶, D. Kisielewska ^{38a}, F. Kiss ⁴⁸, T. Kittelmann ¹²⁴,
 K. Kiuchi ¹⁶¹, E. Kladiva ^{145b}, M. Klein ⁷³, U. Klein ⁷³, K. Kleinknecht ⁸², P. Klimek ^{147a,147b}, A. Klimentov ²⁵,
 R. Klingenberg ⁴³, J.A. Klinger ⁸³, T. Klioutchnikova ³⁰, P.F. Klok ¹⁰⁵, E.-E. Kluge ^{58a}, P. Kluit ¹⁰⁶, S. Kluth ¹⁰⁰,
 E. Kneringer ⁶¹, E.B.F.G. Knoops ⁸⁴, A. Knue ⁵³, D. Kobayashi ¹⁵⁸, T. Kobayashi ¹⁵⁶, M. Kobel ⁴⁴,
 M. Kocian ¹⁴⁴, P. Kodys ¹²⁸, P. Koevesarki ²¹, T. Koffas ²⁹, E. Koffeman ¹⁰⁶, L.A. Kogan ¹¹⁹, S. Kohlmann ¹⁷⁶,
 Z. Kohout ¹²⁷, T. Kohriki ⁶⁵, T. Koi ¹⁴⁴, H. Kolanoski ¹⁶, I. Koletsou ⁵, J. Koll ⁸⁹, A.A. Komar ^{95,*},
 Y. Komori ¹⁵⁶, T. Kondo ⁶⁵, N. Kondrashova ⁴², K. Köneke ⁴⁸, A.C. König ¹⁰⁵, S. König ⁸², T. Kono ^{65,s},
 R. Konoplich ^{109,t}, N. Konstantinidis ⁷⁷, R. Kopeliansky ¹⁵³, S. Koperny ^{38a}, L. Köpke ⁸², A.K. Kopp ⁴⁸,
 K. Korcyl ³⁹, K. Kordas ¹⁵⁵, A. Korn ⁷⁷, A.A. Korol ^{108,c}, I. Korolkov ¹², E.V. Korolkova ¹⁴⁰, V.A. Korotkov ¹²⁹,
 O. Kortner ¹⁰⁰, S. Kortner ¹⁰⁰, V.V. Kostyukhin ²¹, V.M. Kotov ⁶⁴, A. Kotwal ⁴⁵, C. Kourkoumelis ⁹,
 V. Kouskoura ¹⁵⁵, A. Koutsman ^{160a}, R. Kowalewski ¹⁷⁰, T.Z. Kowalski ^{38a}, W. Kozanecki ¹³⁷, A.S. Kozhin ¹²⁹,
 V. Kral ¹²⁷, V.A. Kramarenko ⁹⁸, G. Kramberger ⁷⁴, D. Krasnopevtsev ⁹⁷, M.W. Krasny ⁷⁹,
 A. Krasznahorkay ³⁰, J.K. Kraus ²¹, A. Kravchenko ²⁵, S. Kreiss ¹⁰⁹, M. Kretz ^{58c}, J. Kretzschmar ⁷³,
 K. Kreutzfeldt ⁵², P. Krieger ¹⁵⁹, K. Kroeninger ⁵⁴, H. Kroha ¹⁰⁰, J. Kroll ¹²¹, J. Kroseberg ²¹, J. Krstic ^{13a},
 U. Kruchonak ⁶⁴, H. Krüger ²¹, T. Kruker ¹⁷, N. Krumnack ⁶³, Z.V. Krumshteyn ⁶⁴, A. Kruse ¹⁷⁴,
 M.C. Kruse ⁴⁵, M. Kruskal ²², T. Kubota ⁸⁷, S. Kuday ^{4a}, S. Kuehn ⁴⁸, A. Kugel ^{58c}, A. Kuhl ¹³⁸, T. Kuhl ⁴²,
 V. Kukhtin ⁶⁴, Y. Kulchitsky ⁹¹, S. Kuleshov ^{32b}, M. Kuna ^{133a,133b}, J. Kunkle ¹²¹, A. Kupco ¹²⁶,
 H. Kurashige ⁶⁶, Y.A. Kurochkin ⁹¹, R. Kurumida ⁶⁶, V. Kus ¹²⁶, E.S. Kuwertz ¹⁴⁸, M. Kuze ¹⁵⁸, J. Kvita ¹¹⁴,
 A. La Rosa ⁴⁹, L. La Rotonda ^{37a,37b}, C. Lacasta ¹⁶⁸, F. Lacava ^{133a,133b}, J. Lacey ²⁹, H. Lacker ¹⁶, D. Lacour ⁷⁹,
 V.R. Lacuesta ¹⁶⁸, E. Ladygin ⁶⁴, R. Lafaye ⁵, B. Laforge ⁷⁹, T. Lagouri ¹⁷⁷, S. Lai ⁴⁸, H. Laier ^{58a},
 L. Lambourne ⁷⁷, S. Lammers ⁶⁰, C.L. Lampen ⁷, W. Lampl ⁷, E. Lançon ¹³⁷, U. Landgraf ⁴⁸, M.P.J. Landon ⁷⁵,
 V.S. Lang ^{58a}, A.J. Lankford ¹⁶⁴, F. Lanni ²⁵, K. Lantzsch ³⁰, S. Laplace ⁷⁹, C. Lapoire ²¹, J.F. Laporte ¹³⁷,
 T. Lari ^{90a}, M. Lassnig ³⁰, P. Laurelli ⁴⁷, W. Lavrijsen ¹⁵, A.T. Law ¹³⁸, P. Laycock ⁷³, O. Le Dortz ⁷⁹,
 E. Le Guirieec ⁸⁴, E. Le Menedeu ¹², T. LeCompte ⁶, F. Ledroit-Guillon ⁵⁵, C.A. Lee ¹⁵², H. Lee ¹⁰⁶,
 J.S.H. Lee ¹¹⁷, S.C. Lee ¹⁵², L. Lee ¹⁷⁷, G. Lefebvre ⁷⁹, M. Lefebvre ¹⁷⁰, F. Legger ⁹⁹, C. Leggett ¹⁵, A. Lehan ⁷³,
 M. Lehmacher ²¹, G. Lehmann Miotto ³⁰, X. Lei ⁷, W.A. Leight ²⁹, A. Leisos ¹⁵⁵, A.G. Leister ¹⁷⁷,
 M.A.L. Leite ^{24d}, R. Leitner ¹²⁸, D. Lellouch ¹⁷³, B. Lemmer ⁵⁴, K.J.C. Leney ⁷⁷, T. Lenz ²¹, G. Lenzen ¹⁷⁶,
 B. Lenzi ³⁰, R. Leone ⁷, S. Leone ^{123a,123b}, K. Leonhardt ⁴⁴, C. Leonidopoulos ⁴⁶, S. Leontsinis ¹⁰, C. Leroy ⁹⁴,
 C.G. Lester ²⁸, C.M. Lester ¹²¹, M. Levchenko ¹²², J. Levêque ⁵, D. Levin ⁸⁸, L.J. Levinson ¹⁷³, M. Levy ¹⁸,
 A. Lewis ¹¹⁹, G.H. Lewis ¹⁰⁹, A.M. Leyko ²¹, M. Leyton ⁴¹, B. Li ^{33b,u}, B. Li ⁸⁴, H. Li ¹⁴⁹, H.L. Li ³¹, L. Li ⁴⁵,
 L. Li ^{33e}, S. Li ⁴⁵, Y. Li ^{33c,v}, Z. Liang ¹³⁸, H. Liao ³⁴, B. Liberti ^{134a}, P. Lichard ³⁰, K. Lie ¹⁶⁶, J. Liebal ²¹,
 W. Liebig ¹⁴, C. Limbach ²¹, A. Limosani ⁸⁷, S.C. Lin ^{152,w}, T.H. Lin ⁸², F. Linde ¹⁰⁶, B.E. Lindquist ¹⁴⁹,
 J.T. Linnemann ⁸⁹, E. Lipeles ¹²¹, A. Lipniacka ¹⁴, M. Lisovskyi ⁴², T.M. Liss ¹⁶⁶, D. Lissauer ²⁵, A. Lister ¹⁶⁹,
 A.M. Litke ¹³⁸, B. Liu ¹⁵², D. Liu ¹⁵², J.B. Liu ^{33b}, K. Liu ^{33b,x}, L. Liu ⁸⁸, M. Liu ⁴⁵, M. Liu ^{33b}, Y. Liu ^{33b},
 M. Livan ^{120a,120b}, S.S.A. Livermore ¹¹⁹, A. Lleres ⁵⁵, J. Llorente Merino ⁸¹, S.L. Lloyd ⁷⁵, F. Lo Sterzo ¹⁵²,
 E. Lobodzinska ⁴², P. Loch ⁷, W.S. Lockman ¹³⁸, F.K. Loebinger ⁸³, A.E. Loevschall-Jensen ³⁶, A. Loginov ¹⁷⁷,
 T. Lohse ¹⁶, K. Lohwasser ⁴², M. Lokajicek ¹²⁶, V.P. Lombardo ⁵, B.A. Long ²², J.D. Long ⁸⁸, R.E. Long ⁷¹,
 L. Lopes ^{125a}, D. Lopez Mateos ⁵⁷, B. Lopez Paredes ¹⁴⁰, I. Lopez Paz ¹², J. Lorenz ⁹⁹,
 N. Lorenzo Martinez ⁶⁰, M. Losada ¹⁶³, P. Loscutoff ¹⁵, X. Lou ⁴¹, A. Lounis ¹¹⁶, J. Love ⁶, P.A. Love ⁷¹,
 A.J. Lowe ^{144,f}, F. Lu ^{33a}, N. Lu ⁸⁸, H.J. Lubatti ¹³⁹, C. Luci ^{133a,133b}, A. Lucotte ⁵⁵, F. Luehring ⁶⁰, W. Lukas ⁶¹,
 L. Luminari ^{133a}, O. Lundberg ^{147a,147b}, B. Lund-Jensen ¹⁴⁸, M. Lungwitz ⁸², D. Lynn ²⁵, R. Lysak ¹²⁶,
 E. Lytken ⁸⁰, H. Ma ²⁵, L.L. Ma ^{33d}, G. Maccarrone ⁴⁷, A. Macchiolo ¹⁰⁰, J. Machado Miguens ^{125a,125b},
 D. Macina ³⁰, D. Madaffari ⁸⁴, R. Madar ⁴⁸, H.J. Maddocks ⁷¹, W.F. Mader ⁴⁴, A. Madsen ¹⁶⁷, M. Maeno ⁸,

- T. Maeno 25, E. Magradze 54, K. Mahboubi 48, J. Mahlstedt 106, S. Mahmoud 73, C. Maiani 137,
 C. Maidantchik 24a, A.A. Maier 100, A. Maio 125a, 125b, 125d, S. Majewski 115, Y. Makida 65, N. Makovec 116,
 P. Mal 137,y, B. Malaescu 79, Pa. Malecki 39, V.P. Maleev 122, F. Malek 55, U. Mallik 62, D. Malon 6,
 C. Malone 144, S. Maltezos 10, V.M. Malyshev 108, S. Malyukov 30, J. Mamuzic 13b, B. Mandelli 30,
 L. Mandelli 90a, I. Mandić 74, R. Mandrysch 62, J. Maneira 125a, 125b, A. Manfredini 100,
 L. Manhaes de Andrade Filho 24b, J. Manjarres Ramos 160b, A. Mann 99, P.M. Manning 138,
 A. Manousakis-Katsikakis 9, B. Mansoulie 137, R. Mantifel 86, L. Mapelli 30, L. March 146c, J.F. Marchand 29,
 G. Marchiori 79, M. Marcisovsky 126, C.P. Marino 170, M. Marjanovic 13a, C.N. Marques 125a,
 F. Marroquim 24a, S.P. Marsden 83, Z. Marshall 15, L.F. Marti 17, S. Marti-Garcia 168, B. Martin 30,
 B. Martin 89, T.A. Martin 171, V.J. Martin 46, B. Martin dit Latour 14, H. Martinez 137, M. Martinez 12,o,
 S. Martin-Haugh 130, A.C. Martyniuk 77, M. Marx 139, F. Marzano 133a, A. Marzin 30, L. Masetti 82,
 T. Mashimo 156, R. Mashinistov 95, J. Masik 83, A.L. Maslennikov 108,c, I. Massa 20a, 20b, L. Massa 20a, 20b,
 N. Massol 5, P. Mastrandrea 149, A. Mastroberardino 37a, 37b, T. Masubuchi 156, P. Mättig 176, J. Mattmann 82,
 J. Maurer 26a, S.J. Maxfield 73, D.A. Maximov 108,c, R. Mazini 152, L. Mazzaferro 134a, 134b, G. Mc Goldrick 159,
 S.P. Mc Kee 88, A. McCarn 88, R.L. McCarthy 149, T.G. McCarthy 29, N.A. McCubbin 130, K.W. McFarlane 56,*,
 J.A. McFayden 77, G. Mchedlidze 54, S.J. McMahon 130, R.A. McPherson 170,k, A. Meade 85, J. Mechnick 106,
 M. Medinnis 42, S. Meehan 31, S. Mehlhase 99, A. Mehta 73, K. Meier 58a, C. Meineck 99, B. Meirose 80,
 C. Melachrinos 31, B.R. Mellado Garcia 146c, F. Meloni 17, A. Mengarelli 20a, 20b, S. Menke 100, E. Meoni 162,
 K.M. Mercurio 57, S. Mergelmeyer 21, N. Meric 137, P. Mermod 49, L. Merola 103a, 103b, C. Meroni 90a,
 F.S. Merritt 31, H. Merritt 110, A. Messina 30,z, J. Metcalfe 25, A.S. Mete 164, C. Meyer 82, C. Meyer 121,
 J-P. Meyer 137, J. Meyer 30, R.P. Middleton 130, S. Migas 73, L. Mijović 21, G. Mikenberg 173,
 M. Mikestikova 126, M. Mikuž 74, A. Milic 30, D.W. Miller 31, C. Mills 46, A. Milov 173, D.A. Milstead 147a, 147b,
 D. Milstein 173, A.A. Minaenko 129, I.A. Minashvili 64, A.I. Mincer 109, B. Mindur 38a, M. Mineev 64,
 Y. Ming 174, L.M. Mir 12, G. Mirabelli 133a, T. Mitani 172, J. Mitrevski 99, V.A. Mitsou 168, S. Mitsui 65,
 A. Miucci 49, P.S. Miyagawa 140, J.U. Mjörnmark 80, T. Moa 147a, 147b, K. Mochizuki 84, S. Mohapatra 35,
 W. Mohr 48, S. Molander 147a, 147b, R. Moles-Valls 168, K. Mönig 42, C. Monini 55, J. Monk 36, E. Monnier 84,
 J. Montejo Berlingen 12, F. Monticelli 70, S. Monzani 133a, 133b, R.W. Moore 3, A. Moraes 53, N. Morange 62,
 D. Moreno 82, M. Moreno Llácer 54, P. Morettini 50a, M. Morgenstern 44, M. Morii 57, S. Moritz 82,
 A.K. Morley 148, G. Mornacchi 30, J.D. Morris 75, L. Morvaj 102, H.G. Moser 100, M. Mosidze 51b, J. Moss 110,
 K. Motohashi 158, R. Mount 144, E. Mountricha 25, S.V. Mouraviev 95,* E.J.W. Moyse 85, S. Muanza 84,
 R.D. Mudd 18, F. Mueller 58a, J. Mueller 124, K. Mueller 21, T. Mueller 28, T. Mueller 82, D. Muenstermann 49,
 Y. Munwes 154, J.A. Murillo Quijada 18, W.J. Murray 171, 130, H. Musheghyan 54, E. Musto 153,
 A.G. Myagkov 129, aa, M. Myska 127, O. Nackenhorst 54, J. Nadal 54, K. Nagai 61, R. Nagai 158, Y. Nagai 84,
 K. Nagano 65, A. Nagarkar 110, Y. Nagasaka 59, M. Nagel 100, A.M. Nairz 30, Y. Nakahama 30, K. Nakamura 65,
 T. Nakamura 156, I. Nakano 111, H. Namasivayam 41, G. Nanava 21, R. Narayan 58b, T. Nattermann 21,
 T. Naumann 42, G. Navarro 163, R. Nayyar 7, H.A. Neal 88, P.Yu. Nechaeva 95, T.J. Neep 83, P.D. Nef 144,
 A. Negri 120a, 120b, G. Negri 30, M. Negrini 20a, S. Nektarijevic 49, A. Nelson 164, T.K. Nelson 144,
 S. Nemecek 126, P. Nemethy 109, A.A. Nepomuceno 24a, M. Nessi 30, ab, M.S. Neubauer 166, M. Neumann 176,
 R.M. Neves 109, P. Nevski 25, P.R. Newman 18, D.H. Nguyen 6, R.B. Nickerson 119, R. Nicolaïdou 137,
 B. Nicquevert 30, J. Nielsen 138, N. Nikiforou 35, A. Nikiforov 16, V. Nikolaenko 129, aa, I. Nikolic-Audit 79,
 K. Nikolic 49, K. Nikolopoulos 18, P. Nilsson 8, Y. Ninomiya 156, A. Nisati 133a, R. Nisius 100, T. Nobe 158,
 L. Nodulman 6, M. Nomachi 117, I. Nomidis 29, S. Norberg 112, M. Nordberg 30, O. Novgorodova 44,
 S. Nowak 100, M. Nozaki 65, L. Nozka 114, K. Ntekas 10, G. Nunes Hanninger 87, T. Nunnemann 99,
 E. Nurse 77, F. Nuti 87, B.J. O'Brien 46, F. O'grady 7, D.C. O'Neil 143, V. O'Shea 53, F.G. Oakham 29,e,
 H. Oberlack 100, T. Obermann 21, J. Ocariz 79, A. Ochi 66, I. Ochoa 77, S. Oda 69, S. Odaka 65, H. Ogren 60,
 A. Oh 83, S.H. Oh 45, C.C. Ohm 15, H. Ohman 167, W. Okamura 117, H. Okawa 25, Y. Okumura 31,
 T. Okuyama 156, A. Olariu 26a, A.G. Olchevski 64, S.A. Olivares Pino 46, D. Oliveira Damazio 25,
 E. Oliver Garcia 168, A. Olszewski 39, J. Olszowska 39, A. Onofre 125a, 125e, P.U.E. Onyisi 31, p, C.J. Oram 160a,
 M.J. Oreglia 31, Y. Oren 154, D. Orestano 135a, 135b, N. Orlando 72a, 72b, C. Oropeza Barrera 53, R.S. Orr 159,
 B. Osculati 50a, 50b, R. Ospanov 121, G. Otero y Garzon 27, H. Otono 69, M. Ouchrif 136d, E.A. Ouellette 170,
 F. Ould-Saada 118, A. Ouraou 137, K.P. Oussoren 106, Q. Ouyang 33a, A. Ovcharova 15, M. Owen 83,
 V.E. Ozcan 19a, N. Ozturk 8, K. Pachal 119, A. Pacheco Pages 12, C. Padilla Aranda 12, M. Pagáčová 48,

- S. Pagan Griso 15, E. Paganis 140, C. Pahl 100, F. Paige 25, P. Pais 85, K. Pajchel 118, G. Palacino 160b,
 S. Palestini 30, M. Palka 38b, D. Pallin 34, A. Palma 125a, 125b, J.D. Palmer 18, Y.B. Pan 174,
 E. Panagiotopoulou 10, J.G. Panduro Vazquez 76, P. Pani 106, N. Panikashvili 88, S. Panitkin 25, D. Pantea 26a,
 L. Paolozzi 134a, 134b, Th.D. Papadopoulou 10, K. Papageorgiou 155, A. Paramonov 6,
 D. Paredes Hernandez 34, M.A. Parker 28, F. Parodi 50a, 50b, J.A. Parsons 35, U. Parzefall 48,
 E. Pasqualucci 133a, S. Passaggio 50a, A. Passeri 135a, F. Pastore 135a, 135b,*, Fr. Pastore 76, G. Pásztor 29,
 S. Patarai 176, N.D. Patel 151, J.R. Pater 83, S. Patricelli 103a, 103b, T. Pauly 30, J. Pearce 170, M. Pedersen 118,
 S. Pedraza Lopez 168, R. Pedro 125a, 125b, S.V. Peleganchuk 108, D. Pelikan 167, H. Peng 33b, B. Penning 31,
 J. Penwell 60, D.V. Perepelitsa 25, E. Perez Codina 160a, M.T. Pérez García-Estañ 168, V. Perez Reale 35,
 L. Perini 90a, 90b, H. Pernegger 30, R. Perrino 72a, R. Peschke 42, V.D. Peshekhonov 64, K. Peters 30,
 R.F.Y. Peters 83, B.A. Petersen 30, T.C. Petersen 36, E. Petit 42, A. Petridis 147a, 147b, C. Petridou 155,
 E. Petrolo 133a, F. Petrucci 135a, 135b, N.E. Pettersson 158, R. Pezoa 32b, P.W. Phillips 130, G. Piacquadio 144,
 E. Pianori 171, A. Picazio 49, E. Piccaro 75, M. Piccinini 20a, 20b, R. Piegaia 27, D.T. Pignotti 110, J.E. Pilcher 31,
 A.D. Pilkington 77, J. Pina 125a, 125b, 125d, M. Pinamonti 165a, 165c, ac, A. Pinder 119, J.L. Pinfold 3, A. Pingel 36,
 B. Pinto 125a, S. Pires 79, M. Pitt 173, C. Pizio 90a, 90b, L. Plazak 145a, M.-A. Pleier 25, V. Pleskot 128,
 E. Plotnikova 64, P. Plucinski 147a, 147b, S. Poddar 58a, F. Podlyski 34, R. Poettgen 82, L. Poggioli 116, D. Pohl 21,
 M. Pohl 49, G. Polesello 120a, A. Policicchio 37a, 37b, R. Polifka 159, A. Polini 20a, C.S. Pollard 45,
 V. Polychronakos 25, K. Pommès 30, L. Pontecorvo 133a, B.G. Pope 89, G.A. Popeneciu 26b, D.S. Popovic 13a,
 A. Poppleton 30, X. Portell Bueso 12, S. Pospisil 127, K. Potamianos 15, I.N. Potrap 64, C.J. Potter 150,
 C.T. Potter 115, G. Poulard 30, J. Poveda 60, V. Pozdnyakov 64, P. Pralavorio 84, A. Pranko 15, S. Prasad 30,
 R. Pravahan 8, S. Prell 63, D. Price 83, J. Price 73, L.E. Price 6, D. Prieur 124, M. Primavera 72a, M. Proissl 46,
 K. Prokofiev 47, F. Prokoshin 32b, E. Protopapadaki 137, S. Protopopescu 25, J. Proudfoot 6, M. Przybycien 38a,
 H. Przysiezniak 5, E. Ptacek 115, D. Puddu 135a, 135b, E. Pueschel 85, D. Puldon 149, M. Purohit 25, ad,
 P. Puzo 116, J. Qian 88, G. Qin 53, Y. Qin 83, A. Quadt 54, D.R. Quarrie 15, W.B. Quayle 165a, 165b,
 M. Queitsch-Maitland 83, D. Quilty 53, A. Qureshi 160b, V. Radeka 25, V. Radescu 42, S.K. Radhakrishnan 149,
 P. Radloff 115, P. Rados 87, F. Ragusa 90a, 90b, G. Rahal 179, S. Rajagopalan 25, M. Rammensee 30,
 A.S. Randle-Conde 40, C. Rangel-Smith 167, K. Rao 164, F. Rauscher 99, T.C. Rave 48, T. Ravenscroft 53,
 M. Raymond 30, A.L. Read 118, N.P. Readioff 73, D.M. Rebuzzi 120a, 120b, A. Redelbach 175, G. Redlinger 25,
 R. Reece 138, K. Reeves 41, L. Rehnisch 16, H. Reisin 27, M. Relich 164, C. Rembser 30, H. Ren 33a, Z.L. Ren 152,
 A. Renaud 116, M. Rescigno 133a, S. Resconi 90a, O.L. Rezanova 108.c, P. Reznicek 128, R. Rezvani 94,
 R. Richter 100, M. Ridel 79, P. Rieck 16, J. Rieger 54, M. Rijssenbeek 149, A. Rimoldi 120a, 120b, L. Rinaldi 20a,
 E. Ritsch 61, I. Riu 12, F. Rizatdinova 113, E. Rizvi 75, S.H. Robertson 86, k, A. Robichaud-Veronneau 86,
 D. Robinson 28, J.E.M. Robinson 83, A. Robson 53, C. Roda 123a, 123b, L. Rodrigues 30, S. Roe 30, O. Røhne 118,
 S. Rolli 162, A. Romaniouk 97, M. Romano 20a, 20b, E. Romero Adam 168, N. Rompotis 139, M. Ronzani 48,
 L. Roos 79, E. Ros 168, S. Rosati 133a, K. Rosbach 49, M. Rose 76, P. Rose 138, P.L. Rosendahl 14,
 O. Rosenthal 142, V. Rossetti 147a, 147b, E. Rossi 103a, 103b, L.P. Rossi 50a, R. Rosten 139, M. Rotaru 26a,
 I. Roth 173, J. Rothberg 139, D. Rousseau 116, C.R. Royon 137, A. Rozanov 84, Y. Rozen 153, X. Ruan 146c,
 F. Rubbo 12, I. Rubinskiy 42, V.I. Rud 98, C. Rudolph 44, M.S. Rudolph 159, F. Rühr 48, A. Ruiz-Martinez 30,
 Z. Rurikova 48, N.A. Rusakovich 64, A. Ruschke 99, J.P. Rutherford 7, N. Ruthmann 48, Y.F. Ryabov 122,
 M. Rybar 128, G. Rybkin 116, N.C. Ryder 119, A.F. Saavedra 151, S. Sacerdoti 27, A. Saddique 3, I. Sadeh 154,
 H.F-W. Sadrozinski 138, R. Sadykov 64, F. Safai Tehrani 133a, H. Sakamoto 156, Y. Sakurai 172,
 G. Salamanna 135a, 135b, A. Salamon 134a, M. Saleem 112, D. Salek 106, P.H. Sales De Bruin 139,
 D. Salihagic 100, A. Salnikov 144, J. Salt 168, D. Salvatore 37a, 37b, F. Salvatore 150, A. Salvucci 105,
 A. Salzburger 30, D. Sampsonidis 155, A. Sanchez 103a, 103b, J. Sánchez 168, V. Sanchez Martinez 168,
 H. Sandaker 14, R.L. Sandbach 75, H.G. Sander 82, M.P. Sanders 99, M. Sandhoff 176, T. Sandoval 28,
 C. Sandoval 163, R. Sandstroem 100, D.P.C. Sankey 130, A. Sansoni 47, C. Santoni 34, R. Santonico 134a, 134b,
 H. Santos 125a, I. Santoyo Castillo 150, K. Sapp 124, A. Sapronov 64, J.G. Saraiva 125a, 125d, B. Sarrazin 21,
 G. Sartisohn 176, O. Sasaki 65, Y. Sasaki 156, G. Sauvage 5, *, E. Sauvan 5, P. Savard 159, e, D.O. Savu 30,
 C. Sawyer 119, L. Sawyer 78, n, D.H. Saxon 53, J. Saxon 121, C. Sbarra 20a, A. Sbrizzi 3, T. Scanlon 77,
 D.A. Scannicchio 164, M. Scarcella 151, V. Scarfone 37a, 37b, J. Schaarschmidt 173, P. Schacht 100,
 D. Schaefer 30, R. Schaefer 42, S. Schaepe 21, S. Schaetzle 58b, U. Schäfer 82, A.C. Schaffer 116, D. Schaile 99,
 R.D. Schamberger 149, V. Scharf 58a, V.A. Schegelsky 122, D. Scheirich 128, M. Schernau 164, M.I. Scherzer 35,

- C. Schiavi 50a,50b, J. Schieck 99, C. Schillo 48, M. Schioppa 37a,37b, S. Schlenker 30, E. Schmidt 48,
 K. Schmieden 30, C. Schmitt 82, S. Schmitt 58b, B. Schneider 17, Y.J. Schnellbach 73, U. Schnoor 44,
 L. Schoeffel 137, A. Schoening 58b, B.D. Schoenrock 89, A.L.S. Schorlemmer 54, M. Schott 82, D. Schouten 160a,
 J. Schovancova 25, S. Schramm 159, M. Schreyer 175, C. Schroeder 82, N. Schuh 82, M.J. Schultens 21,
 H.-C. Schultz-Coulon 58a, H. Schulz 16, M. Schumacher 48, B.A. Schumm 138, Ph. Schune 137,
 C. Schwanenberger 83, A. Schwartzman 144, Ph. Schwegler 100, Ph. Schwemling 137, R. Schwienhorst 89,
 J. Schwindling 137, T. Schwindt 21, M. Schwoerer 5, F.G. Sciacca 17, E. Scifo 116, G. Sciolla 23, W.G. Scott 130,
 F. Scuri 123a,123b, F. Scutti 21, J. Searcy 88, G. Sedov 42, E. Sedykh 122, S.C. Seidel 104, A. Seiden 138,
 F. Seifert 127, J.M. Seixas 24a, G. Sekhniaidze 103a, S.J. Sekula 40, K.E. Selbach 46, D.M. Seliverstov 122,*
 G. Sellers 73, N. Semprini-Cesari 20a,20b, C. Serfon 30, L. Serin 116, L. Serkin 54, T. Serre 84, R. Seuster 160a,
 H. Severini 112, T. Sfiligoj 74, F. Sforza 100, A. Sfyrla 30, E. Shabalina 54, M. Shamim 115, L.Y. Shan 33a,
 R. Shang 166, J.T. Shank 22, M. Shapiro 15, P.B. Shatalov 96, K. Shaw 165a,165b, C.Y. Shehu 150, P. Sherwood 77,
 L. Shi 152,ae, S. Shimizu 66, C.O. Shimmin 164, M. Shimojima 101, M. Shiyakova 64, A. Shmeleva 95,
 M.J. Shochet 31, D. Short 119, S. Shrestha 63, E. Shulga 97, M.A. Shupe 7, S. Shushkevich 42, P. Sicho 126,
 O. Sidiropoulou 155, D. Sidorov 113, A. Sidoti 133a, F. Siegert 44, Dj. Sijacki 13a, J. Silva 125a,125d, Y. Silver 154,
 D. Silverstein 144, S.B. Silverstein 147a, V. Simak 127, O. Simard 5, Lj. Simic 13a, S. Simion 116, E. Simioni 82,
 B. Simmons 77, R. Simoniello 90a,90b, M. Simonyan 36, P. Sinervo 159, N.B. Sinev 115, V. Sipica 142,
 G. Siragusa 175, A. Sircar 78, A.N. Sisakyan 64,* S.Yu. Sivoklokov 98, J. Sjölin 147a,147b, T.B. Sjursen 14,
 H.P. Skottowe 57, K.Yu. Skovpen 108, P. Skubic 112, M. Slater 18, T. Slavicek 127, K. Sliwa 162, V. Smakhtin 173,
 B.H. Smart 46, L. Smestad 14, S.Yu. Smirnov 97, Y. Smirnov 97, L.N. Smirnova 98,af, O. Smirnova 80,
 K.M. Smith 53, M. Smizanska 71, K. Smolek 127, A.A. Snesarev 95, G. Snidero 75, S. Snyder 25, R. Sobie 170,k,
 F. Socher 44, A. Soffer 154, D.A. Soh 152,ae, C.A. Solans 30, M. Solar 127, J. Solc 127, E.Yu. Soldatov 97,
 U. Soldevila 168, A.A. Solodkov 129, A. Soloshenko 64, O.V. Solovyanov 129, V. Solovyev 122, P. Sommer 48,
 H.Y. Song 33b, N. Soni 1, A. Sood 15, A. Sopczak 127, B. Sopko 127, V. Sopko 127, V. Sorin 12, M. Sosebee 8,
 R. Soualah 165a,165c, P. Soueid 94, A.M. Soukharev 108,c, D. South 42, S. Spagnolo 72a,72b, F. Spanò 76,
 W.R. Spearman 57, F. Spettel 100, R. Spighi 20a, G. Spigo 30, L.A. Spiller 87, M. Spousta 128, T. Spreitzer 159,
 B. Spurlock 8, R.D. St. Denis 53,* S. Staerz 44, J. Stahlman 121, R. Stamen 58a, S. Stamm 16, E. Stanecka 39,
 R.W. Stanek 6, C. Stanescu 135a, M. Stanescu-Bellu 42, M.M. Stanitzki 42, S. Stapnes 118, E.A. Starchenko 129,
 J. Stark 55, P. Staroba 126, P. Starovoitov 42, R. Staszewski 39, P. Stavina 145a,* P. Steinberg 25, B. Stelzer 143,
 H.J. Stelzer 30, O. Stelzer-Chilton 160a, H. Stenzel 52, S. Stern 100, G.A. Stewart 53, J.A. Stillings 21,
 M.C. Stockton 86, M. Stoebe 86, G. Stoica 26a, P. Stolte 54, S. Stonjek 100, A.R. Stradling 8, A. Straessner 44,
 M.E. Stramaglia 17, J. Strandberg 148, S. Strandberg 147a,147b, A. Strandlie 118, E. Strauss 144, M. Strauss 112,
 P. Strizenec 145b, R. Ströhmer 175, D.M. Strom 115, R. Stroynowski 40, S.A. Stucci 17, B. Stugu 14,
 N.A. Styles 42, D. Su 144, J. Su 124, R. Subramaniam 78, A. Succurro 12, Y. Sugaya 117, C. Suhr 107, M. Suk 127,
 V.V. Sulin 95, S. Sultansoy 4c, T. Sumida 67, S. Sun 57, X. Sun 33a, J.E. Sundermann 48, K. Suruliz 140,
 G. Susinno 37a,37b, M.R. Sutton 150, Y. Suzuki 65, M. Svatos 126, S. Swedish 169, M. Swiatlowski 144,
 I. Sykora 145a, T. Sykora 128, D. Ta 89, C. Taccini 135a,135b, K. Tackmann 42, J. Taenzer 159, A. Taffard 164,
 R. Tafirout 160a, N. Taiblum 154, H. Takai 25, R. Takashima 68, H. Takeda 66, T. Takeshita 141, Y. Takubo 65,
 M. Talby 84, A.A. Talyshев 108,c, J.Y.C. Tam 175, K.G. Tan 87, J. Tanaka 156, R. Tanaka 116, S. Tanaka 132,
 S. Tanaka 65, A.J. Tanasijczuk 143, B.B. Tannenwald 110, N. Tannoury 21, S. Tapprogge 82, S. Tarem 153,
 F. Tarrade 29, G.F. Tartarelli 90a, P. Tas 128, M. Tasevsky 126, T. Tashiro 67, E. Tassi 37a,37b,
 A. Tavares Delgado 125a,125b, Y. Tayalati 136d, F.E. Taylor 93, G.N. Taylor 87, W. Taylor 160b, F.A. Teischinger 30,
 M. Teixeira Dias Castanheira 75, P. Teixeira-Dias 76, K.K. Temming 48, H. Ten Kate 30, P.K. Teng 152,
 J.J. Teoh 117, S. Terada 65, K. Terashi 156, J. Terron 81, S. Terzo 100, M. Testa 47, R.J. Teuscher 159,k,
 J. Therhaag 21, T. Theveneaux-Pelzer 34, J.P. Thomas 18, J. Thomas-Wilske 76, E.N. Thompson 35,
 P.D. Thompson 18, P.D. Thompson 159, R.J. Thompson 83, A.S. Thompson 53, L.A. Thomsen 36,
 E. Thomson 121, M. Thomson 28, W.M. Thong 87, R.P. Thun 88,* F. Tian 35, M.J. Tibbetts 15,
 V.O. Tikhomirov 95,ag, Yu.A. Tikhonov 108,c, S. Timoshenko 97, E. Tiouchichine 84, P. Tipton 177,
 S. Tisserant 84, T. Todorov 5,* S. Todorova-Nova 128, B. Toggerson 7, J. Tojo 69, S. Tokár 145a,
 K. Tokushuku 65, K. Tollefson 89, L. Tomlinson 83, M. Tomoto 102, L. Tompkins 31, K. Toms 104,
 N.D. Topilin 64, E. Torrence 115, H. Torres 143, E. Torró Pastor 168, J. Toth 84,ah, F. Touchard 84, D.R. Tovey 140,
 H.L. Tran 116, T. Trefzger 175, L. Tremblet 30, A. Tricoli 30, I.M. Trigger 160a, S. Trincaz-Duvoud 79,

- M.F. Tripiana ¹², W. Trischuk ¹⁵⁹, B. Trocmé ⁵⁵, C. Troncon ^{90a}, M. Trottier-McDonald ¹⁴³,
 M. Trovatelli ^{135a,135b}, P. True ⁸⁹, M. Trzebinski ³⁹, A. Trzupek ³⁹, C. Tsarouchas ³⁰, J.C.-L. Tseng ¹¹⁹,
 P.V. Tsiareshka ⁹¹, D. Tsionou ¹³⁷, G. Tsipolitis ¹⁰, N. Tsirintanis ⁹, S. Tsiskaridze ¹², V. Tsiskaridze ⁴⁸,
 E.G. Tskhadadze ^{51a}, I.I. Tsukerman ⁹⁶, V. Tsulaia ¹⁵, S. Tsuno ⁶⁵, D. Tsybychev ¹⁴⁹, A. Tudorache ^{26a},
 V. Tudorache ^{26a}, A.N. Tuna ¹²¹, S.A. Tupputi ^{20a,20b}, S. Turchikhin ^{98,af}, D. Turecek ¹²⁷, I. Turk Cakir ^{4d},
 R. Turra ^{90a,90b}, P.M. Tuts ³⁵, A. Tykhanov ⁴⁹, M. Tylmad ^{147a,147b}, M. Tyndel ¹³⁰, K. Uchida ²¹, I. Ueda ¹⁵⁶,
 R. Ueno ²⁹, M. Ughetto ⁸⁴, M. Ugland ¹⁴, M. Uhlenbrock ²¹, F. Ukegawa ¹⁶¹, G. Unal ³⁰, A. Undrus ²⁵,
 G. Unel ¹⁶⁴, F.C. Ungaro ⁴⁸, Y. Unno ⁶⁵, C. Unverdorben ⁹⁹, D. Urbaniec ³⁵, P. Urquijo ⁸⁷, G. Usai ⁸,
 A. Usanova ⁶¹, L. Vacavant ⁸⁴, V. Vacek ¹²⁷, B. Vachon ⁸⁶, N. Valencic ¹⁰⁶, S. Valentini ^{20a,20b},
 A. Valero ¹⁶⁸, L. Valery ³⁴, S. Valkar ¹²⁸, E. Valladolid Gallego ¹⁶⁸, S. Vallecorsa ⁴⁹, J.A. Valls Ferrer ¹⁶⁸,
 W. Van Den Wollenberg ¹⁰⁶, P.C. Van Der Deijl ¹⁰⁶, R. van der Geer ¹⁰⁶, H. van der Graaf ¹⁰⁶,
 R. Van Der Leeuw ¹⁰⁶, D. van der Ster ³⁰, N. van Eldik ³⁰, P. van Gemmeren ⁶, J. Van Nieuwkoop ¹⁴³,
 I. van Vulpen ¹⁰⁶, M.C. van Woerden ³⁰, M. Vanadia ^{133a,133b}, W. Vandelli ³⁰, R. Vanguri ¹²¹,
 A. Vaniachine ⁶, P. Vankov ⁴², F. Vannucci ⁷⁹, G. Vardanyan ¹⁷⁸, R. Vari ^{133a}, E.W. Varnes ⁷, T. Varol ⁸⁵,
 D. Varouchas ⁷⁹, A. Vartapetian ⁸, K.E. Varvell ¹⁵¹, F. Vazeille ³⁴, T. Vazquez Schroeder ⁵⁴, J. Veatch ⁷,
 F. Veloso ^{125a,125c}, T. Velz ²¹, S. Veneziano ^{133a}, A. Ventura ^{72a,72b}, D. Ventura ⁸⁵, M. Venturi ¹⁷⁰,
 N. Venturi ¹⁵⁹, A. Venturini ²³, V. Vercesi ^{120a}, M. Verducci ^{133a,133b}, W. Verkerke ¹⁰⁶, J.C. Vermeulen ¹⁰⁶,
 A. Vest ⁴⁴, M.C. Vetterli ^{143,e}, O. Viazlo ⁸⁰, I. Vichou ¹⁶⁶, T. Vickey ^{146c,ai}, O.E. Vickey Boeriu ^{146c},
 G.H.A. Viehhauser ¹¹⁹, S. Viel ¹⁶⁹, R. Vigne ³⁰, M. Villa ^{20a,20b}, M. Villaplana Perez ^{90a,90b}, E. Vilucchi ⁴⁷,
 M.G. Vinchter ²⁹, V.B. Vinogradov ⁶⁴, J. Virzi ¹⁵, I. Vivarelli ¹⁵⁰, F. Vives Vaque ³, S. Vlachos ¹⁰, D. Vladoiu ⁹⁹,
 M. Vlasak ¹²⁷, A. Vogel ²¹, M. Vogel ^{32a}, P. Vokac ¹²⁷, G. Volpi ^{123a,123b}, M. Volpi ⁸⁷, H. von der Schmitt ¹⁰⁰,
 H. von Radziewski ⁴⁸, E. von Toerne ²¹, V. Vorobel ¹²⁸, K. Vorobev ⁹⁷, M. Vos ¹⁶⁸, R. Voss ³⁰,
 J.H. Vossebeld ⁷³, N. Vranjes ¹³⁷, M. Vranjes Milosavljevic ¹⁰⁶, V. Vrba ¹²⁶, M. Vreeswijk ¹⁰⁶, T. Vu Anh ⁴⁸,
 R. Vuillermet ³⁰, I. Vukotic ³¹, Z. Vykydal ¹²⁷, P. Wagner ²¹, W. Wagner ¹⁷⁶, H. Wahlberg ⁷⁰,
 S. Wahrmund ⁴⁴, J. Wakabayashi ¹⁰², J. Walder ⁷¹, R. Walker ⁹⁹, W. Walkowiak ¹⁴², R. Wall ¹⁷⁷, P. Waller ⁷³,
 B. Walsh ¹⁷⁷, C. Wang ^{152,aj}, C. Wang ⁴⁵, F. Wang ¹⁷⁴, H. Wang ¹⁵, H. Wang ⁴⁰, J. Wang ⁴², J. Wang ^{33a},
 K. Wang ⁸⁶, R. Wang ¹⁰⁴, S.M. Wang ¹⁵², T. Wang ²¹, X. Wang ¹⁷⁷, C. Wanotayaroj ¹¹⁵, A. Warburton ⁸⁶,
 C.P. Ward ²⁸, D.R. Wardrope ⁷⁷, M. Warsinsky ⁴⁸, A. Washbrook ⁴⁶, C. Wasicki ⁴², P.M. Watkins ¹⁸,
 A.T. Watson ¹⁸, I.J. Watson ¹⁵¹, M.F. Watson ¹⁸, G. Watts ¹³⁹, S. Watts ⁸³, B.M. Waugh ⁷⁷, S. Webb ⁸³,
 M.S. Weber ¹⁷, S.W. Weber ¹⁷⁵, J.S. Webster ³¹, A.R. Weidberg ¹¹⁹, P. Weigell ¹⁰⁰, B. Weinert ⁶⁰,
 J. Weingarten ⁵⁴, C. Weiser ⁴⁸, H. Weits ¹⁰⁶, P.S. Wells ³⁰, T. Wenaus ²⁵, D. Wendland ¹⁶, Z. Weng ^{152,ae},
 T. Wengler ³⁰, S. Wenig ³⁰, N. Wermes ²¹, M. Werner ⁴⁸, P. Werner ³⁰, M. Wessels ^{58a}, J. Wetter ¹⁶²,
 K. Whalen ²⁹, A. White ⁸, M.J. White ¹, R. White ^{32b}, S. White ^{123a,123b}, D. Whiteson ¹⁶⁴, D. Wicke ¹⁷⁶,
 F.J. Wickens ¹³⁰, W. Wiedenmann ¹⁷⁴, M. Wielers ¹³⁰, P. Wienemann ²¹, C. Wiglesworth ³⁶,
 L.A.M. Wiik-Fuchs ²¹, P.A. Wijeratne ⁷⁷, A. Wildauer ¹⁰⁰, M.A. Wildt ^{42,ak}, H.G. Wilkens ³⁰, J.Z. Will ⁹⁹,
 H.H. Williams ¹²¹, S. Williams ²⁸, C. Willis ⁸⁹, S. Willocq ⁸⁵, A. Wilson ⁸⁸, J.A. Wilson ¹⁸,
 I. Wingerter-Seez ⁵, F. Winklmeier ¹¹⁵, B.T. Winter ²¹, M. Wittgen ¹⁴⁴, T. Wittig ⁴³, J. Wittkowski ⁹⁹,
 S.J. Wollstadt ⁸², M.W. Wolter ³⁹, H. Wolters ^{125a,125c}, B.K. Wosiek ³⁹, J. Wotschack ³⁰, M.J. Woudstra ⁸³,
 K.W. Wozniak ³⁹, M. Wright ⁵³, M. Wu ⁵⁵, S.L. Wu ¹⁷⁴, X. Wu ⁴⁹, Y. Wu ⁸⁸, E. Wulf ³⁵, T.R. Wyatt ⁸³,
 B.M. Wynne ⁴⁶, S. Xella ³⁶, M. Xiao ¹³⁷, D. Xu ^{33a}, L. Xu ^{33b,al}, B. Yabsley ¹⁵¹, S. Yacoob ^{146b,am}, R. Yakabe ⁶⁶,
 M. Yamada ⁶⁵, H. Yamaguchi ¹⁵⁶, Y. Yamaguchi ¹¹⁷, A. Yamamoto ⁶⁵, K. Yamamoto ⁶³, S. Yamamoto ¹⁵⁶,
 T. Yamamura ¹⁵⁶, T. Yamanaka ¹⁵⁶, K. Yamauchi ¹⁰², Y. Yamazaki ⁶⁶, Z. Yan ²², H. Yang ^{33e}, H. Yang ¹⁷⁴,
 U.K. Yang ⁸³, Y. Yang ¹¹⁰, S. Yanush ⁹², L. Yao ^{33a}, W.-M. Yao ¹⁵, Y. Yasu ⁶⁵, E. Yatsenko ⁴², K.H. Yau Wong ²¹,
 J. Ye ⁴⁰, S. Ye ²⁵, I. Yeletskikh ⁶⁴, A.L. Yen ⁵⁷, E. Yildirim ⁴², M. Yilmaz ^{4b}, R. Yoosoofmiya ¹²⁴, K. Yorita ¹⁷²,
 R. Yoshida ⁶, K. Yoshihara ¹⁵⁶, C. Young ¹⁴⁴, C.J.S. Young ³⁰, S. Youssef ²², D.R. Yu ¹⁵, J. Yu ⁸, J.M. Yu ⁸⁸,
 J. Yu ¹¹³, L. Yuan ⁶⁶, A. Yurkewicz ¹⁰⁷, I. Yusuff ^{28,an}, B. Zabinski ³⁹, R. Zaidan ⁶², A.M. Zaitsev ^{129,aa},
 A. Zaman ¹⁴⁹, S. Zambito ²³, L. Zanello ^{133a,133b}, D. Zanzi ¹⁰⁰, C. Zeitnitz ¹⁷⁶, M. Zeman ¹²⁷, A. Zemla ^{38a},
 K. Zengel ²³, O. Zenin ¹²⁹, T. Ženiš ^{145a}, D. Zerwas ¹¹⁶, G. Zevi della Porta ⁵⁷, D. Zhang ⁸⁸, F. Zhang ¹⁷⁴,
 H. Zhang ⁸⁹, J. Zhang ⁶, L. Zhang ¹⁵², X. Zhang ^{33d}, Z. Zhang ¹¹⁶, Z. Zhao ^{33b}, A. Zhemchugov ⁶⁴,
 J. Zhong ¹¹⁹, B. Zhou ⁸⁸, L. Zhou ³⁵, N. Zhou ¹⁶⁴, C.G. Zhu ^{33d}, H. Zhu ^{33a}, J. Zhu ⁸⁸, Y. Zhu ^{33b}, X. Zhuang ^{33a},
 K. Zhukov ⁹⁵, A. Zibell ¹⁷⁵, D. Ziemińska ⁶⁰, N.I. Zimine ⁶⁴, C. Zimmermann ⁸², R. Zimmermann ²¹,

S. Zimmermann²¹, S. Zimmermann⁴⁸, Z. Zinonos⁵⁴, M. Ziolkowski¹⁴², G. Zobernig¹⁷⁴, A. Zoccoli^{20a,20b}, M. zur Nedden¹⁶, G. Zurzolo^{103a,103b}, V. Zutshi¹⁰⁷, L. Zwalinski³⁰

¹ Department of Physics, University of Adelaide, Adelaide, Australia

² Physics Department, SUNY Albany, Albany, NY, United States

³ Department of Physics, University of Alberta, Edmonton, AB, Canada

⁴ (a) Department of Physics, Ankara University, Ankara; (b) Department of Physics, Gazi University, Ankara; (c) Division of Physics, TOBB University of Economics and Technology, Ankara;

(d) Turkish Atomic Energy Authority, Ankara, Turkey

⁵ LAPP, CNRS/IN2P3 and Université de Savoie, Annecy-le-Vieux, France

⁶ High Energy Physics Division, Argonne National Laboratory, Argonne, IL, United States

⁷ Department of Physics, University of Arizona, Tucson, AZ, United States

⁸ Department of Physics, The University of Texas at Arlington, Arlington, TX, United States

⁹ Physics Department, University of Athens, Athens, Greece

¹⁰ Physics Department, National Technical University of Athens, Zografou, Greece

¹¹ Institute of Physics, Azerbaijan Academy of Sciences, Baku, Azerbaijan

¹² Institut de Física d'Altes Energies and Departament de Física de la Universitat Autònoma de Barcelona, Barcelona, Spain

¹³ (a) Institute of Physics, University of Belgrade, Belgrade; (b) Vinca Institute of Nuclear Sciences, University of Belgrade, Belgrade, Serbia

¹⁴ Department for Physics and Technology, University of Bergen, Bergen, Norway

¹⁵ Physics Division, Lawrence Berkeley National Laboratory and University of California, Berkeley, CA, United States

¹⁶ Department of Physics, Humboldt University, Berlin, Germany

¹⁷ Albert Einstein Center for Fundamental Physics and Laboratory for High Energy Physics, University of Bern, Bern, Switzerland

¹⁸ School of Physics and Astronomy, University of Birmingham, Birmingham, United Kingdom

¹⁹ (a) Department of Physics, Bogazici University, Istanbul; (b) Department of Physics, Dogus University, Istanbul; (c) Department of Physics Engineering, Gaziantep University, Gaziantep, Turkey

²⁰ (a) INFN Sezione di Bologna ; (b) Dipartimento di Fisica e Astronomia, Università di Bologna, Bologna, Italy

²¹ Physikalisches Institut, University of Bonn, Bonn, Germany

²² Department of Physics, Boston University, Boston, MA, United States

²³ Department of Physics, Brandeis University, Waltham, MA, United States

²⁴ (a) Universidade Federal do Rio De Janeiro COPPE/EE/IF, Rio de Janeiro; (b) Electrical Circuits Department, Federal University of Juiz de Fora (UFJF), Juiz de Fora; (c) Federal University of São João do Rei (UFSJ), São João do Rei; (d) Instituto de Física, Universidade de São Paulo, São Paulo, Brazil

²⁵ Physics Department, Brookhaven National Laboratory, Upton, NY, United States

²⁶ (a) National Institute of Physics and Nuclear Engineering, Bucharest; (b) National Institute for Research and Development of Isotopic and Molecular Technologies, Physics Department, Cluj Napoca; (c) University Politehnica Bucharest, Bucharest; (d) West University in Timisoara, Timisoara, Romania

²⁷ Departamento de Física, Universidad de Buenos Aires, Buenos Aires, Argentina

²⁸ Cavendish Laboratory, University of Cambridge, Cambridge, United Kingdom

²⁹ Department of Physics, Carleton University, Ottawa, ON, Canada

³⁰ CERN, Geneva, Switzerland

³¹ Enrico Fermi Institute, University of Chicago, Chicago, IL, United States

³² (a) Departamento de Física, Pontificia Universidad Católica de Chile, Santiago ; (b) Departamento de Física, Universidad Técnica Federico Santa María, Valparaíso, Chile

³³ (a) Institute of High Energy Physics, Chinese Academy of Sciences, Beijing; (b) Department of Modern Physics, University of Science and Technology of China, Anhui ; (c) Department of Physics, Nanjing University, Jiangsu; (d) School of Physics, Shandong University, Shandong; (e) Physics Department, Shanghai Jiao Tong University, Shanghai, China

³⁴ Laboratoire de Physique Corpusculaire, Clermont Université and Université Blaise Pascal and CNRS/IN2P3, Clermont-Ferrand, France

³⁵ Nevis Laboratory, Columbia University, Irvington, NY, United States

³⁶ Niels Bohr Institute, University of Copenhagen, Copenhagen, Denmark

³⁷ (a) INFN Gruppo Collegato di Cosenza, Laboratori Nazionali di Frascati; (b) Dipartimento di Fisica, Università della Calabria, Rende, Italy

³⁸ (a) AGH University of Science and Technology, Faculty of Physics and Applied Computer Science, Krakow; (b) Marian Smoluchowski Institute of Physics, Jagiellonian University, Krakow, Poland

³⁹ The Henryk Niewodniczanski Institute of Nuclear Physics, Polish Academy of Sciences, Krakow, Poland

⁴⁰ Physics Department, Southern Methodist University, Dallas, TX, United States

⁴¹ Physics Department, University of Texas at Dallas, Richardson, TX, United States

⁴² DESY, Hamburg and Zeuthen, Germany

⁴³ Institut für Experimentelle Physik IV, Technische Universität Dortmund, Dortmund, Germany

⁴⁴ Institut für Kern- und Teilchenphysik, Technische Universität Dresden, Dresden, Germany

⁴⁵ Department of Physics, Duke University, Durham, NC, United States

⁴⁶ SUPA – School of Physics and Astronomy, University of Edinburgh, Edinburgh, United Kingdom

⁴⁷ INFN Laboratori Nazionali di Frascati, Frascati, Italy

⁴⁸ Fakultät für Mathematik und Physik, Albert-Ludwigs-Universität, Freiburg, Germany

⁴⁹ Section de Physique, Université de Genève, Geneva, Switzerland

⁵⁰ (a) INFN Sezione di Genova; (b) Dipartimento di Fisica, Università di Genova, Genova, Italy

⁵¹ (a) E. Andronikashvili Institute of Physics, Iv. Javakhishvili Tbilisi State University, Tbilisi ; (b) High Energy Physics Institute, Tbilisi State University, Tbilisi, Georgia

⁵² II Physikalisches Institut, Justus-Liebig-Universität Giessen, Giessen, Germany

⁵³ SUPA – School of Physics and Astronomy, University of Glasgow, Glasgow, United Kingdom

⁵⁴ II Physikalisches Institut, Georg-August-Universität, Göttingen, Germany

⁵⁵ Laboratoire de Physique Subatomique et de Cosmologie, Université Grenoble-Alpes, CNRS/IN2P3, Grenoble, France

⁵⁶ Department of Physics, Hampton University, Hampton, VA, United States

⁵⁷ Laboratory for Particle Physics and Cosmology, Harvard University, Cambridge, MA, United States

⁵⁸ (a) Kirchhoff-Institut für Physik, Ruprecht-Karls-Universität Heidelberg, Heidelberg ; (b) Physikalisches Institut, Ruprecht-Karls-Universität Heidelberg, Heidelberg ; (c) ZITI Institut für technische Informatik, Ruprecht-Karls-Universität Heidelberg, Mannheim, Germany

⁵⁹ Faculty of Applied Information Science, Hiroshima Institute of Technology, Hiroshima, Japan

⁶⁰ Department of Physics, Indiana University, Bloomington, IN, United States

⁶¹ Institut für Astro- und Teilchenphysik, Leopold-Franzens-Universität, Innsbruck, Austria

⁶² University of Iowa, Iowa City, IA, United States

⁶³ Department of Physics and Astronomy, Iowa State University, Ames, IA, United States

⁶⁴ Joint Institute for Nuclear Research, JINR Dubna, Dubna, Russia

⁶⁵ KEK, High Energy Accelerator Research Organization, Tsukuba, Japan

⁶⁶ Graduate School of Science, Kobe University, Kobe, Japan

⁶⁷ Faculty of Science, Kyoto University, Kyoto, Japan

⁶⁸ Kyoto University of Education, Kyoto, Japan

- ⁶⁹ Department of Physics, Kyushu University, Fukuoka, Japan
⁷⁰ Instituto de Física La Plata, Universidad Nacional de La Plata and CONICET, La Plata, Argentina
⁷¹ Physics Department, Lancaster University, Lancaster, United Kingdom
⁷² ^(a) INFN Sezione di Lecce; ^(b) Dipartimento di Matematica e Fisica, Università del Salento, Lecce, Italy
⁷³ Oliver Lodge Laboratory, University of Liverpool, Liverpool, United Kingdom
⁷⁴ Department of Physics, Jožef Stefan Institute and University of Ljubljana, Ljubljana, Slovenia
⁷⁵ School of Physics and Astronomy, Queen Mary University of London, London, United Kingdom
⁷⁶ Department of Physics, Royal Holloway University of London, Surrey, United Kingdom
⁷⁷ Department of Physics and Astronomy, University College London, London, United Kingdom
⁷⁸ Louisiana Tech University, Ruston, LA, United States
⁷⁹ Laboratoire de Physique Nucléaire et de Hautes Energies, UPMC and Université Paris-Diderot and CNRS/IN2P3, Paris, France
⁸⁰ Fysiska institutionen, Lunds universitet, Lund, Sweden
⁸¹ Departamento de Física Teórica C-15, Universidad Autónoma de Madrid, Madrid, Spain
⁸² Institut für Physik, Universität Mainz, Mainz, Germany
⁸³ School of Physics and Astronomy, University of Manchester, Manchester, United Kingdom
⁸⁴ CPPM, Aix-Marseille Université and CNRS/IN2P3, Marseille, France
⁸⁵ Department of Physics, University of Massachusetts, Amherst, MA, United States
⁸⁶ Department of Physics, McGill University, Montreal, QC, Canada
⁸⁷ School of Physics, University of Melbourne, Victoria, Australia
⁸⁸ Department of Physics, The University of Michigan, Ann Arbor, MI, United States
⁸⁹ Department of Physics and Astronomy, Michigan State University, East Lansing, MI, United States
⁹⁰ ^(a) INFN Sezione di Milano; ^(b) Dipartimento di Fisica, Università di Milano, Milano, Italy
⁹¹ B.I. Stepanov Institute of Physics, National Academy of Sciences of Belarus, Minsk, Belarus
⁹² National Scientific and Educational Centre for Particle and High Energy Physics, Minsk, Belarus
⁹³ Department of Physics, Massachusetts Institute of Technology, Cambridge, MA, United States
⁹⁴ Group of Particle Physics, University of Montreal, Montreal, QC, Canada
⁹⁵ P.N. Lebedev Institute of Physics, Academy of Sciences, Moscow, Russia
⁹⁶ Institute for Theoretical and Experimental Physics (ITEP), Moscow, Russia
⁹⁷ National Research Nuclear University MEPhI, Moscow, Russia
⁹⁸ D.V. Skobeltsyn Institute of Nuclear Physics, M.V. Lomonosov Moscow State University, Moscow, Russia
⁹⁹ Fakultät für Physik, Ludwig-Maximilians-Universität München, München, Germany
¹⁰⁰ Max-Planck-Institut für Physik (Werner-Heisenberg-Institut), München, Germany
¹⁰¹ Nagasaki Institute of Applied Science, Nagasaki, Japan
¹⁰² Graduate School of Science and Kobayashi-Maskawa Institute, Nagoya University, Nagoya, Japan
¹⁰³ ^(a) INFN Sezione di Napoli; ^(b) Dipartimento di Fisica, Università di Napoli, Napoli, Italy
¹⁰⁴ Department of Physics and Astronomy, University of New Mexico, Albuquerque, NM, United States
¹⁰⁵ Institute for Mathematics, Astrophysics and Particle Physics, Radboud University Nijmegen/Nikhef, Nijmegen, Netherlands
¹⁰⁶ Nikhef National Institute for Subatomic Physics and University of Amsterdam, Amsterdam, Netherlands
¹⁰⁷ Department of Physics, Northern Illinois University, DeKalb, IL, United States
¹⁰⁸ Budker Institute of Nuclear Physics, SB RAS, Novosibirsk, Russia
¹⁰⁹ Department of Physics, New York University, New York, NY, United States
¹¹⁰ Ohio State University, Columbus, OH, United States
¹¹¹ Faculty of Science, Okayama University, Okayama, Japan
¹¹² Homer L. Dodge Department of Physics and Astronomy, University of Oklahoma, Norman, OK, United States
¹¹³ Department of Physics, Oklahoma State University, Stillwater, OK, United States
¹¹⁴ Palacký University, RCPTM, Olomouc, Czech Republic
¹¹⁵ Center for High Energy Physics, University of Oregon, Eugene, OR, United States
¹¹⁶ LAL, Université Paris-Sud and CNRS/IN2P3, Orsay, France
¹¹⁷ Graduate School of Science, Osaka University, Osaka, Japan
¹¹⁸ Department of Physics, University of Oslo, Oslo, Norway
¹¹⁹ Department of Physics, Oxford University, Oxford, United Kingdom
¹²⁰ ^(a) INFN Sezione di Pavia; ^(b) Dipartimento di Fisica, Università di Pavia, Pavia, Italy
¹²¹ Department of Physics, University of Pennsylvania, Philadelphia, PA, United States
¹²² Petersburg Nuclear Physics Institute, Gatchina, Russia
¹²³ ^(a) INFN Sezione di Pisa; ^(b) Dipartimento di Fisica E. Fermi, Università di Pisa, Pisa, Italy
¹²⁴ Department of Physics and Astronomy, University of Pittsburgh, Pittsburgh, PA, United States
¹²⁵ ^(a) Laboratorio de Instrumentacao e Física Experimental de Partículas – LIP, Lisboa; ^(b) Faculdade de Ciências, Universidade de Lisboa, Lisboa; ^(c) Department of Physics, University of Coimbra, Coimbra; ^(d) Centro de Física Nuclear da Universidade de Lisboa, Lisboa; ^(e) Departamento de Física, Universidade do Minho, Braga; ^(f) Departamento de Física Teórica y del Cosmos and CAFPE, Universidad de Granada, Granada (Spain); ^(g) Dep Física and CEFITEC of Faculdade de Ciencias e Tecnologia, Universidade Nova de Lisboa, Caparica, Portugal
¹²⁶ Institute of Physics, Academy of Sciences of the Czech Republic, Praha, Czech Republic
¹²⁷ Czech Technical University in Prague, Praha, Czech Republic
¹²⁸ Faculty of Mathematics and Physics, Charles University in Prague, Praha, Czech Republic
¹²⁹ State Research Center Institute for High Energy Physics, Protvino, Russia
¹³⁰ Particle Physics Department, Rutherford Appleton Laboratory, Didcot, United Kingdom
¹³¹ Physics Department, University of Regina, Regina, SK, Canada
¹³² Ritsumeikan University, Kusatsu, Shiga, Japan
¹³³ ^(a) INFN Sezione di Roma; ^(b) Dipartimento di Fisica, Sapienza Università di Roma, Roma, Italy
¹³⁴ ^(a) INFN Sezione di Roma Tor Vergata; ^(b) Dipartimento di Fisica, Università di Roma Tor Vergata, Roma, Italy
¹³⁵ ^(a) INFN Sezione di Roma Tre; ^(b) Dipartimento di Matematica e Fisica, Università Roma Tre, Roma, Italy
¹³⁶ ^(a) Faculté des Sciences Ain Chock, Réseau Universitaire de Physique des Hautes Energies – Université Hassan II, Casablanca; ^(b) Centre National de l'Energie des Sciences Techniques Nucléaires, Rabat; ^(c) Faculté des Sciences Semlalia, Université Cadi Ayyad, LPHEA, Marrakech; ^(d) Faculté des Sciences, Université Mohamed Premier and LPTPM, Oujda; ^(e) Faculté des sciences, Université Mohammed V-Agdal, Rabat, Morocco
¹³⁷ DSM/IRFU (Institut de Recherches sur les Lois Fondamentales de l'Univers), CEA Saclay (Commissariat à l'Energie Atomique et aux Energies Alternatives), Gif-sur-Yvette, France
¹³⁸ Santa Cruz Institute for Particle Physics, University of California Santa Cruz, Santa Cruz, CA, United States
¹³⁹ Department of Physics, University of Washington, Seattle, WA, United States
¹⁴⁰ Department of Physics and Astronomy, University of Sheffield, Sheffield, United Kingdom
¹⁴¹ Department of Physics, Shinshu University, Nagano, Japan
¹⁴² Fachbereich Physik, Universität Siegen, Siegen, Germany
¹⁴³ Department of Physics, Simon Fraser University, Burnaby, BC, Canada

- 144 SLAC National Accelerator Laboratory, Stanford, CA, United States
 145 ^(a) Faculty of Mathematics, Physics & Informatics, Comenius University, Bratislava ; ^(b) Department of Subnuclear Physics, Institute of Experimental Physics of the Slovak Academy of Sciences, Kosice, Slovak Republic
 146 ^(a) Department of Physics, University of Cape Town, Cape Town; ^(b) Department of Physics, University of Johannesburg, Johannesburg, ^(c) School of Physics, University of the Witwatersrand, Johannesburg, South Africa
 147 ^(a) Department of Physics, Stockholm University; ^(b) The Oskar Klein Centre, Stockholm, Sweden
 148 Physics Department, Royal Institute of Technology, Stockholm, Sweden
 149 Departments of Physics & Astronomy and Chemistry, Stony Brook University, Stony Brook, NY, United States
 150 Department of Physics and Astronomy, University of Sussex, Brighton, United Kingdom
 151 School of Physics, University of Sydney, Sydney, Australia
 152 Institute of Physics, Academia Sinica, Taipei, Taiwan
 153 Department of Physics, Technion: Israel Institute of Technology, Haifa, Israel
 154 Raymond and Beverly Sackler School of Physics and Astronomy, Tel Aviv University, Tel Aviv, Israel
 155 Department of Physics, Aristotle University of Thessaloniki, Thessaloniki, Greece
 156 International Center for Elementary Particle Physics and Department of Physics, The University of Tokyo, Tokyo, Japan
 157 Graduate School of Science and Technology, Tokyo Metropolitan University, Tokyo, Japan
 158 Department of Physics, Tokyo Institute of Technology, Tokyo, Japan
 159 Department of Physics, University of Toronto, Toronto, ON, Canada
 160 ^(a) TRIUMF, Vancouver, BC; ^(b) Department of Physics and Astronomy, York University, Toronto, ON, Canada
 161 Faculty of Pure and Applied Sciences, University of Tsukuba, Tsukuba, Japan
 162 Department of Physics and Astronomy, Tufts University, Medford, MA, United States
 163 Centro de Investigaciones, Universidad Antonio Narino, Bogota, Colombia
 164 Department of Physics and Astronomy, University of California Irvine, Irvine, CA, United States
 165 ^(a) INFN Gruppo Collegato di Udine, Sezione di Trieste, Udine; ^(b) ICTP, Trieste; ^(c) Dipartimento di Chimica, Fisica e Ambiente, Università di Udine, Udine, Italy
 166 Department of Physics, University of Illinois, Urbana, IL, United States
 167 Department of Physics and Astronomy, University of Uppsala, Uppsala, Sweden
 168 Instituto de Física Corpuscular (IFIC) and Departamento de Física Atómica, Molecular y Nuclear and Departamento de Ingeniería Electrónica and Instituto de Microelectrónica de Barcelona (IMB-CNM), University of Valencia and CSIC, Valencia, Spain
 169 Department of Physics, University of British Columbia, Vancouver, BC, Canada
 170 Department of Physics and Astronomy, University of Victoria, Victoria, BC, Canada
 171 Department of Physics, University of Warwick, Coventry, United Kingdom
 172 Waseda University, Tokyo, Japan
 173 Department of Particle Physics, The Weizmann Institute of Science, Rehovot, Israel
 174 Department of Physics, University of Wisconsin, Madison, WI, United States
 175 Fakultät für Physik und Astronomie, Julius-Maximilians-Universität, Würzburg, Germany
 176 Fachbereich C Physik, Bergische Universität Wuppertal, Wuppertal, Germany
 177 Department of Physics, Yale University, New Haven, CT, United States
 178 Yerevan Physics Institute, Yerevan, Armenia
 179 Centre de Calcul de l’Institut National de Physique Nucléaire et de Physique des Particules (IN2P3), Villeurbanne, France

^a Also at Department of Physics, King's College London, London, United Kingdom.

^b Also at Institute of Physics, Azerbaijan Academy of Sciences, Baku, Azerbaijan.

^c Also at Novosibirsk State University, Novosibirsk, Russia.

^d Also at Particle Physics Department, Rutherford Appleton Laboratory, Didcot, United Kingdom.

^e Also at TRIUMF, Vancouver, BC, Canada.

^f Also at Department of Physics, California State University, Fresno, CA, United States.

^g Also at Department of Physics, University of Fribourg, Fribourg, Switzerland.

^h Also at Tomsk State University, Tomsk, Russia.

ⁱ Also at CPPM, Aix-Marseille Université and CNRS/IN2P3, Marseille, France.

^j Also at Università di Napoli Parthenope, Napoli, Italy.

^k Also at Institute of Particle Physics (IPP), Canada.

^l Also at Department of Physics, St. Petersburg State Polytechnical University, St. Petersburg, Russia.

^m Also at Chinese University of Hong Kong, China.

ⁿ Also at Louisiana Tech University, Ruston, LA, United States.

^o Also at Institutio Catalana de Recerca i Estudis Avancats, ICREA, Barcelona, Spain.

^p Also at Department of Physics, The University of Texas at Austin, Austin, TX, United States.

^q Also at Institute of Theoretical Physics, Ilia State University, Tbilisi, Georgia.

^r Also at CERN, Geneva, Switzerland.

^s Also at Ochadai Academic Production, Ochanomizu University, Tokyo, Japan.

^t Also at Manhattan College, New York, NY, United States.

^u Also at Institute of Physics, Academia Sinica, Taipei, Taiwan.

^v Also at LAL, Université Paris-Sud and CNRS/IN2P3, Orsay, France.

^w Also at Academia Sinica Grid Computing, Institute of Physics, Academia Sinica, Taipei, Taiwan.

^x Also at Laboratoire de Physique Nucléaire et de Hautes Energies, UPMC and Université Paris-Diderot and CNRS/IN2P3, Paris, France.

^y Also at School of Physical Sciences, National Institute of Science Education and Research, Bhubaneswar, India.

^z Also at Dipartimento di Fisica, Sapienza Università di Roma, Roma, Italy.

^{aa} Also at Moscow Institute of Physics and Technology State University, Dolgoprudny, Russia.

^{ab} Also at Section de Physique, Université de Genève, Geneva, Switzerland.

^{ac} Also at International School for Advanced Studies (SISSA), Trieste, Italy.

^{ad} Also at Department of Physics and Astronomy, University of South Carolina, Columbia, SC, United States.

^{ae} Also at School of Physics and Engineering, Sun Yat-sen University, Guangzhou, China.

^{af} Also at Faculty of Physics, M.V. Lomonosov Moscow State University, Moscow, Russia.

^{ag} Also at National Research Nuclear University MEPhI, Moscow, Russia.

^{ah} Also at Institute for Particle and Nuclear Physics, Wigner Research Centre for Physics, Budapest, Hungary.

^{ai} Also at Department of Physics, Oxford University, Oxford, United Kingdom.

^{aj} Also at Department of Physics, Nanjing University, Jiangsu, China.

^{ak} Also at Institut für Experimentalphysik, Universität Hamburg, Hamburg, Germany.

^{al} Also at Department of Physics, The University of Michigan, Ann Arbor, MI, United States.

^{am} Also at Discipline of Physics, University of KwaZulu-Natal, Durban, South Africa.

^{an} Also at University of Malaya, Department of Physics, Kuala Lumpur, Malaysia.

* Deceased.